Scaling of quantum Fisher information for quantum exceptional point sensors

Chun-Hui Liu,[1,2] Fu Li,[3] Shengwang Du,[2,4,5] Jianming Wen,[6] Lan Yang,[3] and Chuanwei Zhang[1,2,*]

[1]*Department of Physics, Washington University, St. Louis, MO 63130, USA*
[2]*Department of Physics, The University of Texas at Dallas, Richardson, Texas 75080, USA*
[3]*Department of Electrical and Systems Engineering, Washington University, St. Louis, MO 63130, USA*
[4]*Elmore Family School of Electrical and Computer Engineering, Purdue University, West Lafayette, IN 47907*
[5]*Department of Physics and Astronomy, Purdue University, West Lafayette, IN 47907*
[6]*Department of Physics, Kennesaw State University, Marietta, GA 30060, USA*

In recent years, significant progress has been made in utilizing the divergence of spectrum response rate at the exceptional point (EP) for sensing in classical systems, while the use and characterization of quantum EPs for sensing have been largely unexplored. For a quantum EP sensor, an important issue is the relation between the order of the quantum EP and the scaling of quantum Fisher information (QFI), an essential quantity for characterizing quantum sensors. Here we investigate multi-mode quadratic bosonic systems, which exhibit higher-order EP dynamics, but possess Hermitian Hamiltonians without Langevin noise, thus can be utilized for quantum sensing. We derive an exact analytic formula for the QFI, from which we establish a scaling relation between the QFI and the order of the EP. We apply the formula to study a three-mode EP sensor and a multi-mode bosonic Kitaev chain and show that the EP physics can significantly enhance the sensing sensitivity. Our work establishes the connection between two important fields: non-Hermitian EP dynamics and quantum sensing, and may find important applications in quantum information and quantum non-Hermitian physics.

arXiv:2404.03803v1 [quant-ph] 4 Apr 2024

Introduction. — Exceptional points (EPs), the degenerate points of non-Hermitian systems where two or more eigenstates coalesce [1–4], have recently emerged as a novel platform for achieving high precision sensing of physical parameters [5–21]. In a classical system, the high sensitivity stems from the scaling of the eigenspectrum $\sim \omega^{1/2}$ of a typical second-order (*i.e.*, two-fold degeneracy) EP, leading to a divergent spectrum response rate $d(\Delta\omega)/d\epsilon \propto \epsilon^{-1/2}$ under a perturbation ϵ of a physical parameter deviated from the EP [5, 8]. For a higher ($M \geq 3$) order EP with $\Delta\omega \sim \epsilon^{d_\omega}$ ($d_\omega \geq 1/M$), the divergence can be more substantial $\sim \epsilon^{1/M-1}$ to achieve higher sensitivity [9, 12, 15].

While the EP-based sensing is well studied in classical open systems like gain/loss nanophotonics, its generalization to a quantum system poses a fundamental challenge [16–18, 22–27]. In an open quantum system, the intrinsic Langevin noises may break the underlying symmetry (e.g., parity-time) that protects the EP, rendering the conceptual difficulty for even defining EP-based quantum sensor [27]. Recently, it was shown in a two-mode bosonic parametric amplification process, an EP could emerge from the dynamical evolution matrix of the Hermitian quadratic bosonic Hamiltonian, thus avoids Langevin noise [20, 21]. Around the EP, the quantum dynamics are very sensitive to the small perturbation of the parameter, therefore can be utilized as a quantum EP sensor [21].

The emergence of the quantum EP in the two-mode bosonic Hamiltonian and its application in quantum sensing naturally raise questions about the general EP physics and the characterization of EP-based quantum sensors in multi-mode quadratic bosonic Hamiltonians, which have been experimentally engineered in nonlinear optical media [28, 29], multi-frequency superconducting parametric cavities [30, 31], and optomechanical systems [32–34] in recent years. In quantum sensing, quantum Fisher information (QFI) is one main characteristic quantity that provides a low bound for sensing precision through quantum Cramér-Rao bound [35, 36]. QFI is very different from the divergence of the spectrum response rate that characterizes classical EP-based sensors. It is unclear how the scaling of the quantum EP spectrum is connected with the behavior of the QFI and whether there exists certain universal scaling of the QFI at/around the EP.

To address these questions, we study the QFI in a generic multi-mode bosonic quadratic Hamiltonian, which is Hermitian but its Heisenberg equation of motion (HEOM) is governed by a non-Hermitian dynamical matrix [37–39], yielding the EP physics. Our main results are:

i) We derive an analytic formula of the QFI that is generally hard to calculate even numerically for multi-mode quadratic Hamiltonians due to the exponentially large Hilbert space of particle numbers. Current methods for the estimate of QFI relies on approximate the input-out theory in quantum optics [19, 40], instead of the direct evaluation over the quantum wavefunction. We further explore of the applications of the analytic formula in a three-mode quantum sensor as well as the multi-mode bosonic Kitaev chain.

ii) Utilizing the analytic formula, we find a universal scaling of the QFI $F(t) \sim t^{d_F}$ with $d_F \leq 4M-2$ at an M-th order EP for a large time t, which establishes the connection between the QFI and the order of the EP. From the analytic formula and scaling relation, we show: 1) EP can significantly enhance the sensitivity: the achievable

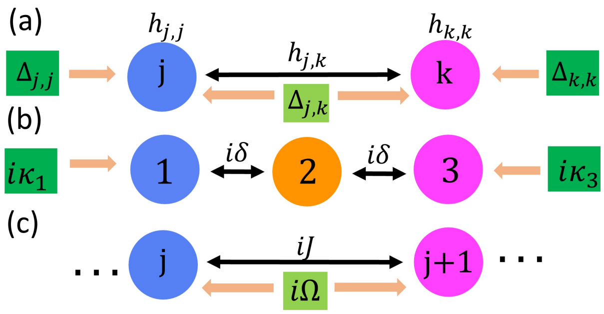

FIG. 1. (a) Schematic diagram of different terms in the generic Hamiltonian (1). (b) and (c) illustrate the three mode model and bosonic Kitaev chain, respectively.

t^{4M-2} scaling showcases the QFI can grow much faster over time than non-EP sensors with typically $\sim t^2$ scaling; 2) Different from the divergence of the spectrum response rate, there is no divergence of the QFI at EP due to the continuity of the QFI formula, therefore the large EP sensitivity enhancement can be achieved for parameters close to the EP.

iii) In an N-mode bosonic Kitaev chain, near the EP the QFI per particle at a fixed time has an exponential scaling $F(t) \sim \beta^{2N-2}$ ($\beta > 1$ depends on parameters of the Kitaev chain), which indicates the sensitivity of quantum EP sensor can increase exponentially with the system size, paving the way for designing novel quantum EP sensors through size/mode engineering.

Analytic formula for QFI: Consider a generic N-mode Hermitian bosonic quadratic Hamiltonian (*i.e.*, Bogoliubov Hamiltonian),

$$\hat{H} = \sum_{j,k=1}^{N} (h_{j,k}\hat{a}_j^\dagger \hat{a}_k + \frac{\Delta_{j,k}}{2}\hat{a}_j^\dagger \hat{a}_k^\dagger + \frac{\Delta_{j,k}^*}{2}\hat{a}_j \hat{a}_k), \quad (1)$$

where $\hat{a}_k$ is the bosonic annihilation operator, $h_{j,k} = h_{k,j}^*$, $\Delta_{j,k} = \Delta_{k,j}$ due to the Hermiticity of $\hat{H}$ and bosonic commutation relation. A schematic diagram of different terms in the Hamiltonian is shown in Fig. 1(a). The Heisenberg equation of motion (HEOM) is $i\frac{d}{dt}\hat{V}(t) = H_D\hat{V}(t)$, where $\hat{V}(t) = \left[\ A,\ \ A^\dagger\ \right]^T$, $A = (\hat{a}_1, ..., \hat{a}_N)$, T is the transpose operator,

$$H_D = \begin{pmatrix} h & \Delta \\ -\Delta^* & -h^* \end{pmatrix} \quad (2)$$

is the dynamical matrix, h and Δ are $N \times N$ matrices. H_D satisfies the symmetries $\tau_x H_D \tau_x = -H_D^*$, $\tau_z H_D \tau_z = H_D^\dagger$ and $\tau_y H_D \tau_y = -H_D^{\mathbf{T}}$ [41–45], where τ_x, τ_y, and τ_z are Pauli matrices. According to HEOM, we have $\hat{V}(t) = e^{-iH_D t}\hat{V}(0) = S(t)\hat{V}(0)$.

In terms of the real and imaginary parts of h and Δ, the dynamical matrix can be written as

$$H_D = \tau_0 \otimes ih_I + \tau_z \otimes h_R + \tau_x \otimes i\Delta_I + i\tau_y \otimes \Delta_R, \quad (3)$$

where $h_I^T = -h_I$, $h_R^T = h_R$, $\Delta_I^T = \Delta_I$, $\Delta_R^T = \Delta_R$ are all real matrices. H_D generally does not possess EPs (e.g., $\Delta = 0$ and H_D is Hermitian), and the EPs may exist when both h and Δ are nonzero. In the presence of certain symmetry of H_D, the $2N \times 2N$ dynamical matrix can be block diagonalized into two $N \times N$ matrices. For instance, when $h_R = \Delta_R = 0$ (e.g., the three-mode and Kitaev chain shown below), H_D satisfies a symmetry $[H_D, \tau_x] = 0$, allowing the block diagonalization of H_D. In each block, the EP is determined by the corresponding block matrix, but the maximum order of EPs $M \leq N$.

We consider a N-mode coherent initial state given by $|\psi_0\rangle = |\alpha_1, ..., \alpha_N\rangle = \hat{D}_1(\alpha_1)...\hat{D}_N(\alpha_N)|0\rangle$ with $\hat{D}_j(\alpha_j) = e^{\alpha_j \hat{a}_j^\dagger - \alpha_j^* \hat{a}_j}$. The quantum state at time t becomes $|\psi_t\rangle = e^{-i\hat{H}t}|\psi_0\rangle$. With a tedious calculation, we find the QFI $F_\eta = 4[\langle \partial_\eta \psi_t | \partial_\eta \psi_t\rangle - |\langle \psi_t | \partial_\eta \psi_t\rangle|^2]$ for a sensing parameter η is [46]

$$F_\eta = 4\boldsymbol{B}^\dagger \boldsymbol{B} + 2\mathrm{Tr}[\boldsymbol{C}_2^\dagger \boldsymbol{C}_2], \quad (4)$$

where $\boldsymbol{B} = \boldsymbol{C}_1\boldsymbol{\alpha} + \boldsymbol{C}_2\boldsymbol{\alpha}^*$, $\boldsymbol{\alpha} = [\alpha_1, ..., \alpha_N]^{\mathrm{T}}$ and $\boldsymbol{C}_1$ and $\boldsymbol{C}_2$ are $N \times N$ matrices given by

$$\begin{pmatrix} \boldsymbol{C}_1 & \boldsymbol{C}_2 \\ \boldsymbol{C}_2^* & \boldsymbol{C}_1^* \end{pmatrix} = \int_{y=0}^{t} dy [S(y)]^\dagger \Sigma_z \partial_\eta H_D S(y), \quad (5)$$

where $\Sigma_z = \tau_z \otimes \mathbb{I}$, $S(y) = e^{-iyH_D}$, $\mathbb{I}$ is the $N \times N$ identity matrix.

Eqs. (4) and (5) also apply to time-dependent systems with $S(y) = \mathcal{T}[exp(-i\int_{x=0}^{y} dx H_D(x))]$ for time-dependent dynamical matrix $H_D(t)$, where $\mathcal{T}$ is the time ordering operator. The QFI formula for other initial states beyond coherent states is given in the supplementary materials [46].

The scaling of the QFI with time can be derived from Eq. (4). At an M-th order EP, when the imaginary parts of the eigenvalues of H_D are equal to zero (i.e., stable region), there always exists at least one matrix element in $S(y) = e^{-iyH_D}$, whose leading order is proportional to y^{M-1} [2]. According to Eq. (5), the leading matrix elements of $\boldsymbol{C}_1$ and $\boldsymbol{C}_2$ are proportional to t^{2M-1} except for accidental parameter regions where the coefficient cancellation leads to lower order of t dependence. Hence $F_\eta(t) \sim t^{d_F}$ with $d_F \leq 4M-2$, and the maximum $d_F = 4M-2$ can be achieved for general parameter regions. In contrast, for a Hermitian Hamiltonian, S_y is purely a phase and $C_j \sim t$, thus the QFI is $\sim t^2$.

The above results can be better illustrated with a simple single mode ($N = 1$) Hamiltonian

$$\hat{H}_1 = \delta\hat{a}^\dagger\hat{a} + i\frac{\kappa}{2}(\hat{a}^{\dagger 2} - \hat{a}^2), \quad (6)$$

where the dynamical matrix $H_{D1} = \delta\tau_z + i\kappa\tau_x$. κ is the single mode squeezing parameter, and δ is the phase mismatch. H_{D1} obeys the anti-$\mathcal{PT}$ symmetry $\{H_{D1}, \mathcal{PT}\} = 0$ with $\mathcal{P} = \tau_x$ and $\mathcal{T} = \mathcal{K}$, and possesses a second order ($M = 2$) EP at $\delta = \kappa$. The energy spectrum response $\Delta\omega_{\pm} = \pm(\delta\epsilon)^{1/2}$ for a perturbation $\epsilon = \delta - \kappa$ from the EP for the parameter κ. At the EP, the time evolution matrix $S(t) = \begin{pmatrix} 1 - it\delta & t\delta \\ t\delta & 1 + it\delta \end{pmatrix}$ with the leading order $\sim t^{M-1} = t$. For the sensing parameter κ, $\partial_\kappa H_{D1} = i\tau_x$, $\Sigma_z = \tau_z$, and the resulting $C_1 = -4\delta^2 t^3/3$ and $C_2 = -2i\delta^2 t^3/3 + \delta^2 t^2 + it$, with the leading order $\sim t^{2M-1} = t^3$. Therefore the QFI scales as $F_\kappa = 4|C_1\alpha + C_2\alpha^*|^2 + 2|C_2|^2 \sim t^6$ with $d_F = 4M - 2 = 6$ as predicted by the scaling law. Hereafter, we apply the analytic formula and the scaling law to two complex multi-mode examples: a three mode sensor and a multi-mode Kitaev chain.

Three mode quantum EP sensor.— Three coupled optical cavities with gain/neutral/loss pattern exhibit a third order EP with enhanced sensitivity, as demonstrated in recent experiments [9]. Here we consider a similar three mode Hamiltonian

$$\hat{H}_3 = i\delta\hat{a}_1^\dagger\hat{a}_2 + i\delta\hat{a}_2^\dagger\hat{a}_3 + \frac{i\kappa_1}{2}\hat{a}_1^2 + \frac{i\kappa_3}{2}\hat{a}_3^{\dagger 2} + \text{h.c.}, \quad (7)$$

where the gain/loss pattern is replaced by the single mode squeezing in modes 1 and 3, as illustrated in Fig. 1(b). The dynamical matrix can be written as $H_{D3} = \tau_0 \otimes \mathbf{K}_1 + \tau_x \otimes \mathbf{K}_2$ with $\mathbf{K}_1 = -\delta(\lambda_2 + \lambda_7)$, $\mathbf{K}_2 = \text{diag}[-i\kappa_1, 0, i\kappa_3]$, and λ_2 and λ_7 being Gell-Mann matrices [47]. As discussed previously, the τ_x symmetry allows the diagonalization of H_{D3} into two irreducible blocks $H_{D3\pm} = \mathbf{K}_1 \pm \mathbf{K}_2$. $H_{D3\pm}$ can be regarded as the quantum generalization of the gain/neutral/loss cavity model [9].

Each block exhibits a third-order ($M = 3$) EP at $\sqrt{2}\delta = \kappa_1 = \kappa_3$ with three degenerate eigenvalues $\omega_k^{\pm} = 0$ for $k = 1, 2, 3$. Consider a perturbation of $\kappa_1 = \sqrt{2}\delta + \epsilon$ ($\epsilon << \delta$) from the EP for mode 1, the spectrum response $\Delta\omega_k^{\pm} = \omega_k^{\pm}(\epsilon) - \omega_k^{\pm}(0) = ie^{\pm i\pi k/3}\delta^{2/3}\epsilon^{1/3}$ at the leading order, showing a $\epsilon^{1/3}$ scaling behavior (i.e., the exponent $d_\omega = 1/3$) [46], similar as that for classical coupled cavities [9]. In Fig. 2(a), we plot the numerical results for the maximum spectrum response $\Delta\omega_{\kappa_1} = \max_{\pm,k}|\Delta\omega_k^{\pm}|$ with respect to ϵ (red triangles) and the linear fitting $\ln(\Delta\omega_{\kappa_1}) = 0.33\ln(\epsilon) + 0.01$ (black solid line), showing excellent agreement with the analytic result.

For quantum sensing of the parameter κ_1, we find $F_{\kappa_1} \propto t^{10}$ when $t \to +\infty$ from Eq. (4) [46] for a coherent initial state. In Fig. 2(b), we show the numerical result of $\ln(F_{\kappa_1})$ as a function of $\ln(t)$, and its linear fitting $\ln(F_{\kappa_1}) = 10\ln(t) - 3.22$, showing the numerical result agrees well with our analytical prediction [46]. $d_F = 4M - 2 = 10$ reaches the maximum exponent of the scaling. Far from the EP with $\kappa_1 = \kappa_3 = 0$, $F_{\kappa_1} \propto t^2$ when $t \to +\infty$ [46], similar as that for a Hermitian sensor. The t^2 to t^{10} scaling change of the QFI demonstrates the EP-enhanced sensitivity.

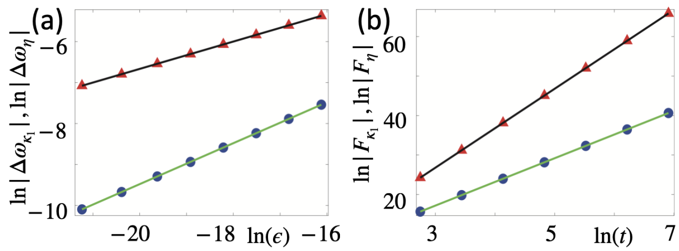

FIG. 2. Maximum spectrum response and QFI for the three mode model. Parameters $\delta = 1$ and $\kappa_1 = \kappa_3 = \sqrt{2}$ for the EP. (a) Plot of maximum spectrum responses versus the perturbation ϵ. (b) Plot of QFI versus time t. In (a) and (b), the red triangles and blue dots are numerical results without and with constraint $\kappa_1 = \kappa_3 = \eta$, respectively. The solid lines are fitting functions.

Different perturbations for the same EP may induce different spectrum responses, leading to different scalings of the QFI. In the three mode Hamiltonian (7), a constraint $\kappa_1 = \kappa_3 = \eta$ with a perturbation $\eta = \sqrt{2}\delta + \epsilon$ for both modes 1 and 3 around the third order EP $\eta = \sqrt{2}\delta$ leads to the double degenerate spectrum response $\Delta\omega_1^{\pm} = 0$, $\Delta\omega_2^{\pm} = i\sqrt{2\sqrt{2}\delta\epsilon}$, and $\Delta\omega_3^{\pm} = -i\sqrt{2\sqrt{2}\delta\epsilon}$. They have the $\epsilon^{1/2}$ scaling, agreeing with the numerical result and its fitting line $\ln(\Delta\omega_\eta) = 0.5\ln(\epsilon) + 0.51$ in Fig. 2(a), where $\Delta\omega_\eta = \max_{\pm,k}|\Delta\omega_k^{\pm}|$ for the perturbation in η. The QFI $F_\eta \propto t^6$ when $t \to +\infty$ [46], which also shows excellent agreement with the numerical result and its linear fitting $\ln(F_\eta) = 6\ln(t) - 0.82$ in Fig. 2(b). Here $d_F = 6 < 4M - 2$ and $d_\omega = 1/2 > 1/M$.

Bosonic Kitaev chain— We extend the analysis from three modes to N modes and consider the bosonic Kitaev chain with the Hamiltonian [19, 38, 48]

$$\hat{H}_{BKC} = \sum_{j=1}^{N-1}\left(iJ\hat{a}_j^\dagger\hat{a}_{j+1} + i\Omega\hat{a}_j^\dagger\hat{a}_{j+1}^\dagger + \text{h.c.}\right). \quad (8)$$

The dynamical matrix for the HEOM $H_{DK} = \tau_0 \otimes \mathbf{L}_1 + \tau_x \otimes \mathbf{L}_2$, where $\mathbf{L}_1$ and $\mathbf{L}_2$ are $N \times N$ matrices with $(\mathbf{L}_1)_{j,j+1} = -(\mathbf{L}_1)_{j+1,j} = iJ$ and $(\mathbf{L}_2)_{j,j+1} = (\mathbf{L}_2)_{j+1,j} = i\Omega$ (all other elements are 0). The model is schematically illustrated in Fig. 1(c). Under unitary transformation $(\tau_x, \tau_y, \tau_z) \to (\tau_z, \tau_y, -\tau_x)$, H_{DK} can be block diagonalized as $\tau_0 \otimes \mathbf{L}_1 + \tau_z \otimes \mathbf{L}_2$ with $H_{DK+} = \mathbf{L}_1 + \mathbf{L}_2$ and $H_{DK-} = \mathbf{L}_1 - \mathbf{L}_2$ being two irreducible blocks that represent Hatano-Nelson model [49]. At $J = \Omega$, both blocks $H_{DK\pm}$ reduce to the N-dimensional Jordan normal forms with zero eigenvalues in the diagonal, yielding two degenerate N-th order (*i.e.*, $M = N$) EPs.

A perturbation from the EP $\epsilon = J - \Omega$ leads to the change of the $2N$ eigenvalues

$$\Delta\omega_k = 2\sqrt{(2J - \epsilon)\epsilon}\cos\left(\frac{k\pi}{N+1}\right) \quad (9)$$

for $k = 1, ..., N$, which are double degenerate for two blocks. Clearly, $\Delta\omega_k = 0$ for $k = (N+1)/2$ with an odd

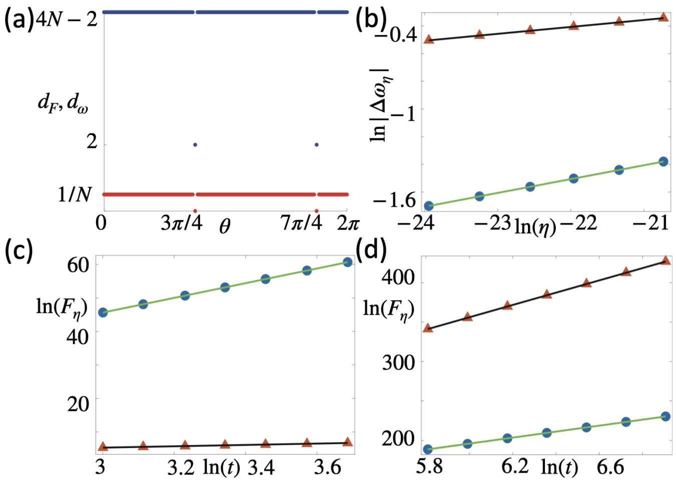

FIG. 3. Maximum spectrumn response and QFI of bosonic Kitaev chain at $J = \Omega = 1$. (a) Schematic diagram of the exponents d_F (blue) and d_ω (red) versus θ. (b) Maximum spectrum response versus $\ln(\eta)$. The red triangles (blue dots) are numerical results of $\ln(\Delta\omega_\eta)$ for $N = 20$ (10). (c) The red triangles (blue dots) are numerical results of QFI versus $\ln(t)$ for $\theta = 3\pi/4$ ($\theta = 2.99\pi/4$). $\eta = 0$ and $N = 6$. (d) QFI versus $\ln(t)$. The red triangles (blue dots) are numerical results of $\ln(F_\eta)$ for $N = 20$ (10). The solid lines in (b-d) are fitting functions.

N, while all other spectrum responses $\Delta\omega_k \propto \epsilon^{1/2}$ do not reach the maximum scaling $\epsilon^{1/N}$. The QFI $F_\Omega \propto t^{4j+2}$ for both $N = 2j$ and $2j + 1$, indicating each non-zero $\sqrt{\epsilon}$ spectrum may contribute t^2 scaling of QFI. The scaling factor $d_F = 4j + 2 < d_F^{\max} = 4M - 2$.

In order to reach the maximum spectrum response exponent $d_\omega = 1/N$, we consider a local perturbation

$$\hat{H}_\eta = i\eta \left[\sin(\theta)\hat{a}_N^\dagger \hat{a}_1 + \cos(\theta)\hat{a}_N^\dagger \hat{a}_1^\dagger\right] + \text{h.c.} \tag{10}$$

that couples modes 1 and N. $\hat{H}_\eta$ adds $(\mathbf{L}_1)_{N,1} = -(\mathbf{L}_1)_{1,N} = i\eta\sin(\theta)$ and $(\mathbf{L}_2)_{N,1} = (\mathbf{L}_2)_{1,N} = i\eta\cos(\theta)$ in the dynamical matrix. We find the maximum spectrum response $\Delta\omega_\eta = \max_k(|\Delta\omega_k|) \propto \eta^{1/N}$ (i.e., $d_\omega = 1/N$) for $\theta \neq \frac{3\pi}{4}$ and $\frac{7\pi}{4}$, while $\Delta\omega_\eta = 0$ (i.e., $d_\omega = 0$) for $\theta = \frac{3\pi}{4}$ or $\frac{7\pi}{4}$ [46]. From Eq. (4), we find $F_\eta \propto t^{4N-2}$ (i.e., $d_F = 4N - 2$) for $\theta \neq \frac{3\pi}{4}$ and $\frac{7\pi}{4}$, and $F_\eta \propto t^2$ (i.e., $d_F = 2$) for $\theta = \frac{3\pi}{4}$ or $\frac{7\pi}{4}$ [46] when $t \to \infty$. In Fig. 3(a), we illustrate d_F and d_ω as a function of θ at the EP $J = \Omega = 1$ and $\eta = 0$.

The analytical results are confirmed by the numerical calculations. In Fig. 3(b), we plot the numerical maximum spectrum response with respect to the perturbation η around the EP $J = \Omega = 1$ for the system size $N = 20$ and 10), together with their fittings $\ln(\Delta\omega_\eta) = 0.05\ln(\eta) + 0.69$ and $\ln(\Delta\omega_\eta) = 0.1\ln(\eta) + 0.69$. They agree well with the analytical expressions for the response exponent $1/N$ shown in Fig. 3(a). In Fig. 3(c), we plot $\ln(F_\eta)$ versus $\ln(t)$ for $N = 6$ at the EP with $\eta = 0$ for slightly different $\theta = 3\pi/4$ and $\theta = 2.99\pi/4$. The fitting functions are found to be $\ln(\Delta\omega_\eta) = 2.02\ln(t) - 0.74$ and $\ln(\Delta\omega_\eta) = 21.92\ln(t) - 20.14$, respectively. The result confirms the t^2 scaling of the QFI at the accidental degenerate point $\theta = 3\pi/4$. In Fig. 3(d), we plot $\ln(F_\eta)$ versus $\ln(t)$ at the EP for two different system sizes $N = 20$ and 10, with their linear fitting functions $\ln(F_\eta) = 77.93\ln(t) - 111.49$ and $\ln(F_\eta) = 37.97\ln(t) - 31.89$. We see they satisfy $d_F = 4N - 2$, reaching the maximum scaling exponent for the QFI.

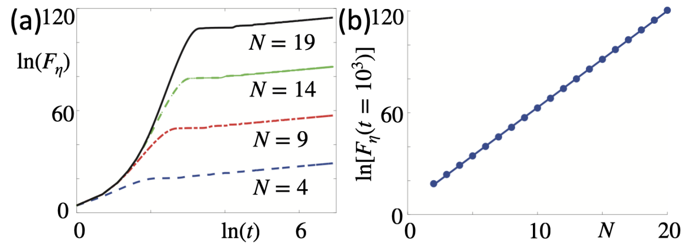

FIG. 4. The parameters are $J = 1$, $\Omega = 0.9$, and $\eta = 0$. (a) QFI $\ln(F_\eta)$ versus $\ln(t)$ for $N = 4, 9, 14, 19$. (b) Fixed time logarithm QFI $\ln[F_\eta(t_0 = 1000)]$ versus size N. The blue dots are numerical results and the solid line is the fitting function.

Far from the EP with $J \neq 0$ and $\eta = \Omega = 0$, we find $F_\eta \propto t^2$ when $t \to +\infty$ from Eq. (4). Therefore our analytical and numerical results demonstrate the enhanced quantum sensitivity at the EP (from t^2 to t^{4N-2}). The Kitaev chain model also indicates that the maximum scaling t^{4M-2} can be reached for an M-th order EP when the dynamical matrix can transform to the Jordan normal form.

At an N-th order EP and with a fixed large time $t = t_0$, F_η is proportional to t_0^{4N-2} at the leading order, indicating the sensitivity may be exponentially enhanced by the system size. However, such t_0 may approach infinity exactly at the EP. Since the QFI is a continuous function of time and other parameters, the enhanced sensitivity at the EP may pass to the nearby interval around the EP, where t_0 is finite. We consider the parameters near the EP with $\eta = 0$, $\beta = \sqrt{\frac{J+\Omega}{J-\Omega}} \gg 1$ and a fixed but finite large time t_0. We can diagonalize the dynamical matrix H_{DK} with a unitary matrix and find that $F_\eta(t = t_0)$ is proportional to β^{4N-4} at the leading order, *i.e.*, $\ln(F_\eta(t = t_0))$ is approximately proportional to $4N\ln(\beta)$.

In Fig. 4(a), we plot the numerical calculation of $\ln(F_\eta)$ as a function of $\ln(t)$ for $N = 4, 9, 14, 19$, with parameters $J = 1$, $\Omega = 0.9$, $\theta = \pi/4$, and $\eta = 0$. We see the growth of QFI with time becomes polynomial after certain time, indicating the saturation of the initial exponential growth due to the finite size of the system. In fact, in a periodic Kitaev chain, the parameter $J = 1$ and $\Omega = 0.9$ yields imaginary eigenspectrum, leading to the exponential growth of the QFI with time. However, the finite size spectrum is still real, leading to the saturation of QFI after the boundary effect kicks in. In Fig. 4(b), we show the numerical calculation of $\ln(F_\eta)$ with respect to N at a fixed time $t_0 = 1000$, with the fitting equation $\ln[F_\eta(t = 1000)] = 5.69N + 6.17$. The numerical coefficient 5.69 is consistent with theoretical coefficient $4\ln(\beta) \approx 5.89$.

Finally, the leading term of total particle number $Q = \langle\psi_t|\sum_{j=1}^{N} \hat{a}_j^\dagger \hat{a}_j|\psi_t\rangle$ scales as $Q \sim \beta^{2N-2}$, therefore the QFI at the fixed time reaches the Heisenberg limit with $F_\eta \sim Q^2$, indicating the QFI per particle is exponentially enhanced. Such exponentially enhanced sensitivity may originate from the non-Hermitian skin effect (NHSE). In the bosonic Kitaev chain, there is an NHSE for H_{DK} without the perturbation η, leading to the accumulation of the wavefunction at the boundary. However, the boundary coupling from the perturbation η leads to the disappearance of the NHSE, which causes a dramatic change of the wavefunction and energy spectrum, yielding the exponential enhancement of the QFI per particle [11]. This reveals that previous conclusion that NHSE cannot be used to enhance per-particle sensitivity [19] based on the input-out theory may be model dependent.

Conclusion and discussion. — In this Letter, we derive the exact QFI formula for a generic quadratic Bosonic Hamiltonian. Utilizing the exact formula, we establish the connection between the QFI scaling exponent and the order of EP of the dynamical matrix. Our analytic methods can also be applied to other important models, e.g., quadratic bosonic Hamiltonian with topological bands [11, 39], for studying quantum squeezing, entanglement and sensing of topological multi-mode chains. While our work on the QFI establishes the lower bound for the ultimate precision for quantum EP sensors, the optimal strategies for achieving such bound are unknown and demand developing well-designed measurement schemes [50]. Our result bridges the fields of quantum sensing and non-Hermitian EP physics and may be useful for the design of new EP-based quantum sensors.

Acknowledgement: We thank the helpful discussions with Q. Zhuang and X. Zhao. C.L. and C.Z. are supported by AFOSR (FA9550-20-1-0220) and NSF (PHY-2409943, OMR-2228725, ECC-2411394). J.W. and D.S. are supported by DOE (DE-SC0022069). J.W. is also support by NSF (OMR-2329027). L.Y. acknowledges support from the McKelvey School of Engineering at Washington University in St. Louis.

* chuanwei.zhang@wustl.edu

[1] C. M. Bender and S. Boettcher, Real Spectra in Non-Hermitian Hamiltonians Having $\mathscr{PT}$ Symmetry, Phys. Rev. Lett. **80**, 5243 (1998).

[2] Y. Ashida, Z. Gong, and Masahito Ueda, Non-Hermitian Physics, Advances in Physics **69**, 3 (2020).

[3] E. J. Bergholtz, J. C. Budich, and F. K. Kunst, Exceptional Topology of Non-Hermitian Systems, Rev. Mod. Phys. **93**, 15005 (2021).

[4] S. K. Ozdemir, S. Rotter, F. Nori, and L. Yang, Parity-time symmetry and exceptional points in photonics, Nat. Photon. **18**, 783 (2019)

[5] J. Wiersig, Enhancing the Sensitivity of Frequency and Energy Splitting Detection by Using Exceptional Points: Application to Microcavity Sensors for Single-Particle Detection, Phys. Rev. Lett. **112**, 203901 (2014).

[6] L. Feng, Z. J. Wong, R.-M. Ma, Y. Wang, and X. Zhang, Single-mode laser by parity-time symmetry breaking, Science **346**, 972 (2014).

[7] Z.-P. Liu, J. Zhang, Ş. K. Özdemir, B. Peng, H. Jing, X.-Y. Lü, C.-W. Li, L. Yang, F. Nori, and Y.-x. Liu, Metrology with $\mathcal{PT}$-Symmetric Cavities: Enhanced Sensitivity near the $\mathcal{PT}$-Phase Transition, Phys. Rev. Lett. **117**, 110802 (2016).

[8] W. Chen, Ş. K. Özdemir, G. Zhao, J. Wiersig, and L. Yang, Exceptional points enhance sensing in an optical microcavity, Nature **548**, 192 (2017).

[9] H. Hodaei, A. U. Hassan, S. Wittek, H. Garcia-Gracia, R. El-Ganainy, D. N. Christodoulides, Enhanced sensitivity at higher-order exceptional points, Nature **548**, 187 (2017).

[10] C. Chen, L. Jin, and R.-B. Liu, Sensitivity of parameter estimation near the exceptional point of a non-Hermitian system, New J. Phys. **21**, 083002 (2019).

[11] J. C. Budich and E. J. Bergholtz, Non-Hermitian Topological Sensors, Phys. Rev. Lett. **125**, 180403 (2020).

[12] Z. Lin, A. Pick, M. Lončar, and A. W. Rodriguez, Enhanced Spontaneous Emission at Third-Order Dirac Exceptional Points in Inverse-Designed Photonic Crystals, Phys. Rev. Lett. **117**, 107402 (2016).

[13] R. Kononchuk, J. Cai, F. Ellis, R. Thevamaran, and T. Kottos, Exceptional-point-based accelerometers with enhanced signal-to-noise ratio, Nature **607**, 697 (2022).

[14] H. Hodaei, M.-A. Miri, M. Heinrich, D. N. Christodoulides, and M. Khajavikhan, Parity-time–symmetric microring lasers, Science **346**, 975 (2014).

[15] Z. Xiao, H. Li, T. Kottos, and A. Alù, Enhanced Sensing and Nondegraded Thermal Noise Performance Based on $\mathcal{PT}$-Symmetric Electronic Circuits with a Sixth-Order Exceptional Point, Phys. Rev. Lett. **123**, 213901 (2019).

[16] W. Langbein, No exceptional precision of exceptional-point sensors, Phys. Rev. A **98**, 023805 (2018).

[17] M. Zhang, W. Sweeney, C. W. Hsu, L. Yang, A. D. Stone, and L. Jiang, Quantum Noise Theory of Exceptional Point Amplifying Sensors, Phys. Rev. Lett. **123**, 180501 (2019).

[18] H.-K. Lau and A. A. Clerk, Fundamental limits and non-reciprocal approaches in non-Hermitian quantum sensing, Nat. Commun. **9**, 4320 (2018).

[19] A. McDonald and A. A. Clerk, Exponentially-enhanced quantum sensing with non-Hermitian lattice dynamics, Nat. Commun. **11**, 5382 (2020).

[20] Y.-X. Wang and A. A. Clerk, Non-Hermitian dynamics without dissipation in quantum systems, Phys. Rev. A **99**, 063834 (2019).

[21] X.-W. Luo, C. Zhang, and S. Du, Quantum Squeezing and Sensing with Pseudo-Anti-Parity-Time Symmetry, Phys. Rev. Lett. **128**, 173602 (2022).

[22] Y. Choi, C. Hahn, J.W. Yoon, S.H. Song, and P. Berini, Extremely broadband, on-chip optical nonreciprocity enabled by mimicking nonlinear anti-adiabatic quantum jumps near exceptional points, Nat. Commun. **8**, 14154

(2017).
[23] Y. Chu, Y. Liu, H. Liu, and J. Cai, Quantum Sensing with a Single-Qubit Pseudo-Hermitian System, Phys. Rev. Lett. **124**, 020501 (2020).
[24] M. Naghiloo, M. Abbasi, Y.N. Joglekar, and K.W. Murch, Quantum state tomography across the exceptional point in a single dissipative qubit, Nat. Phys. 15, 1232 (2019).
[25] Y. Wu, W. Liu, J. Geng, X. Song, X. Ye, C.-K. Duan, X. Rong, and J. Du, Observation of parity-time symmetry breaking in a single-spin system, Science 364, 878 (2019).
[26] S. Yu et al., Experimental Investigation of Quantum PTEnhanced Sensor, Phys. Rev. Lett. **125**, 240506 (2020).
[27] S. Scheel and A. Szameit, PT-symmetric photonic quantum systems with gain and loss do not exist, Europhys. Lett. 122, 34001 (2018).
[28] H. Wang, C. Fabre, and J. Jing, Single-step fabrication of scalable multimode quantum resources using four-wave mixing with a spatially structured pump, Phys. Rev. A **95**, 051802 (2017).
[29] K. Zhang, W. Wang, S. Liu, X. Pan, J. Du, Y. Lou, S. Yu, S. Lv, N. Treps, C. Fabre, and J. Jing, Reconfigurable hexapartite entanglement by spatially multiplexed four-wave mixing processes, Phys. Rev. Lett. **124**, 090501 (2020).
[30] J. H. Busnaina, Z. Shi, A. McDonald, D. Dubyna, I. Nsanzineza, Jimmy S. C. Hung, C. W. Sandbo Chang, A. A. Clerk, C. M. Wilson, Quantum Simulation of the Bosonic Kitaev Chain,arXiv:2309.06178 (2023).
[31] C. Gaikwad, D. Kowsari, W. Chen, K. W. Murch, Observing Parity Time Symmetry Breaking in a Josephson Parametric Amplifier, Phys. Rev. Research **5**, L042024 (2023).
[32] C. C. Wanjura, J. J. Slim, J. del Pino, M. Brunelli, E. Verhagen, and A. Nunnenkamp, Quadrature nonreciprocity in bosonic networks without breaking time-reversal symmetry, Nat. Phys. **19**, 1429 (2023).
[33] J. d. Pino, J. J. Slim, and E. Verhagen, Non-Hermitian chiral phononics through optomechanically induced squeezing, Nature **606**, 82 (2022).
[34] J. J. Slim, C. C. Wanjura, M. Brunelli, J. d. Pino, A. Nunnenkamp, E. Verhagen, Optomechanical realization of the bosonic Kitaev-Majorana chain, arXiv:2309.05825 (2023).
[35] L. Pezzè, A. Smerzi, M. K. Oberthaler, R. Schmied, and P. Treutlein, Quantum metrology with nonclassical states of atomic ensembles, Rev. Mod. Phys. **90**, 035005 (2018).
[36] C. L. Degen, F. Reinhard, and P. Cappellaro, Quantum sensing, Rev. Mod. Phys. **89**, 035002 (2017).
[37] S. Lieu, Topological symmetry classes for non-Hermitian models and connections to the bosonic Bogoliubov–de Gennes equation, Phys. Rev. B **98**, 115135 (2018).
[38] A. McDonald, T. Pereg-Barnea, and A. A. Clerk, Phase-Dependent Chiral Transport and Effective Non-Hermitian Dynamics in a Bosonic Kitaev-Majorana Chain, Phys. Rev. X **8**, 041031 (2018).
[39] L.-L. Wan and X.-Y. Lü, Quantum-Squeezing-Induced Point-Gap Topology and Skin Effect, Phys. Rev. Lett. **130**, 203605 (2023).
[40] A. A. Clerk, M. H. Devoret, S. M. Girvin, Florian Marquardt, and R. J. Schoelkopf, Introduction to quantum noise, measurement, and amplification, Rev. Mod. Phys. **82**, 1155 (2010).
[41] D. Bernard and A. LeClair, A classification of non-Hermitian random matrices, in *Statistical Field Theories*, edited by A. Cappelli and G. Mussardo (Springer Netherlands, Dordrecht, 2002) pp. 207-214.
[42] K. Kawabata, K. Shiozaki, M. Ueda, and M. Sato, Symmetry and Topology in Non-Hermitian Physics, Phys. Rev. X **9**, 041015 (2019).
[43] H. Zhou and J. Y. Lee, Periodic table for topological bands with non-Hermitian symmetries, Phys. Rev. B **99**, 235112 (2019).
[44] C.-H. Liu and S. Chen, Topological classification of defects in non-Hermitian systems, Phys. Rev. B **100**, 144106 (2019).
[45] C.-H. Liu, H. Hu, and S. Chen, Symmetry and topological classification of Floquet non-Hermitian systems, Phys. Rev. B **105**, 214305 (2022).
[46] See supplemental materials for the derivation of general QFI formula, single-mode model, three-mode model, and bosonic Kitaev chain.
[47] M. Gell-Mann, Symmetries of Baryons and Mesons, Phys. Rev. **125**, 1067 (1962).
[48] A. Y. Kitaev, Unpaired Majorana fermions in quantum wires, Physics-Uspekhi **44**, 131 (2001).
[49] N. Hatano and D. R. Nelson, Localization Transitions in Non-Hermitian Quantum Mechanics, Phys. Rev. Lett. **77**, 570 (1996).
[50] Z. Zhang and Q. Zhuang, Distributed Quantum Sensing, Quantum Sci. Technol. **6**, 043001 (2021).

SI. DERIVATION OF THE ANALYTIC FORMULA FOR QUANTUM FISHER INFORMATION

A. QFI for coherent initial state and time-independent Hamiltonian

In this section, we derive the quantum Fisher information (QFI) formula for a sensing parameter η in a generic multimode bosonic quadratic Hamiltonian

$$\hat{H} = \sum_{j,k=1}^{N} (h_{j,k}\hat{a}_j^\dagger \hat{a}_k + \frac{\Delta_{j,k}}{2}\hat{a}_j^\dagger \hat{a}_k^\dagger + \frac{\Delta_{j,k}^*}{2}\hat{a}_j \hat{a}_k), \tag{S1}$$

where $h_{j,k} = h_{k,j}^*$, $\Delta_{j,k} = \Delta_{k,j}$, and $\hat{a}_k$ is the bosonic annihilation operator satisfying the bosonic commutation relations $[a_j, a_k] = 0$ and $\left[a_j^\dagger, a_k\right] = \delta_{jk}$. The Hamiltonian is Hermitian and reduces to the well-known tight-binding model when $\Delta = 0$. The Heisenberg equation of motion (HEOM) is

$$\frac{d\hat{a}_j(t)}{dt} = i[\hat{H}, \hat{a}_j(t)] = i\sum_k [-h_{j,k}\hat{a}_k(t) - \Delta_{j,k}\hat{a}_k^\dagger(t)], \tag{S2}$$

which can be rewritten as

$$i\frac{d}{dt}\hat{V}(t) = H_D\hat{V}(t). \tag{S3}$$

with

$$H_D = \begin{pmatrix} h & \Delta \\ -\Delta^* & -h^* \end{pmatrix}, \tag{S4}$$

$$\hat{V}(t) = [\hat{a}_1(t), \hat{a}_2(t), ..., \hat{a}_N(t), \hat{a}_1^\dagger(t), \hat{a}_2^\dagger(t), ..., \hat{a}_N^\dagger(t)]^T, \tag{S5}$$

h and Δ being $N \times N$ matrices. H_D is the *dynamical matrix*, instead of the Hamiltonian matrix. H_D satisfies $\tau_x H_D \tau_x = -H_D^*$, $\tau_z H_D \tau_z = H_D^\dagger$ and $\tau_y H_D \tau_y = -H_D^{\mathbf{T}}$, where τ_x, τ_y, and τ_z are Pauli matrices.

According to HEOM, we have

$$\hat{V}(t) = e^{-iH_D t}\hat{V}(0) = S(t)\hat{V}(0), \tag{S6}$$

where

$$S(t) = e^{-iH_D t}. \tag{S7}$$

Thus the time evolution of the field operators becomes

$$\hat{a}_j(t) = \sum_{k=1}^{N} \left(P_{j,k}(t)\hat{a}_k(0) + Q_{j,k}(t)\hat{a}_k^\dagger(0) \right), \tag{S8}$$

where $P_{j,k}(t) = S_{j,k}(t)$, $Q_{j,k}(t) = S_{j,(k+N)}(t)$, and $j = 1, 2, ..., N$. For convenience, we use $\hat{a}_k$ and $\hat{a}_k^\dagger$ to represent $\hat{a}_k(0)$ and $\hat{a}_k^\dagger(0)$, respectively.

In this section, we consider a coherent initial state

$$|\psi_0\rangle = |\alpha_1, \alpha_2, ..., \alpha_N\rangle = \hat{D}_1(\alpha_1)\hat{D}_2(\alpha_2)...\hat{D}_N(\alpha_N)|0\rangle,$$

where

$$\hat{D}_j(\alpha_j) = e^{\alpha_j \hat{a}_j^\dagger - \alpha_j^* \hat{a}_j}.$$

The QFI is defined as

$$F_\eta\left(t\right) = 4[\langle\partial_\eta\psi_t||\partial_\eta\psi_t\rangle - |\langle\psi_t||\partial_\eta\psi_t\rangle|^2],$$

which requires the evaluation of the quantum state at time t

$$|\psi_t\rangle = e^{-i\hat{H}t}|\psi_0\rangle.$$

Inset the coherent initial state in, we have

$$|\partial_\eta\psi_t\rangle = \partial_\eta e^{-i\hat{H}t}\hat{D}_1(\alpha_1)\hat{D}_2(\alpha_2)...\hat{D}_N(\alpha_N)|0\rangle.$$

The derivative with the sensing parameter η is only applied to the term $e^{-i\hat{H}t}$ with

$$\begin{aligned}
&\partial_\eta e^{-i\hat{H}t}\\
=&\int_{x=0}^{1} dx\cdot e^{-i\hat{H}t(1-x)}\partial_\eta(-i\hat{H}t)e^{-i\hat{H}tx}\\
=&-it\int_{x=0}^{1} dx\cdot e^{-i\hat{H}t(1-x)}\partial_\eta\left[\sum_{m,n=1}^{N}(h_{m,n}\hat{a}_m^\dagger\hat{a}_n+\frac{\Delta_{m,n}}{2}\hat{a}_m^\dagger\hat{a}_n^\dagger+\frac{\Delta_{m,n}^*}{2}\hat{a}_m\hat{a}_n)\right]e^{-i\hat{H}tx}\\
=&\sum_{m,n=1}^{N}-ite^{-i\hat{H}t}\int_{x=0}^{1} dx\cdot e^{i\hat{H}tx}\left(\partial_\eta h_{m,n}\hat{a}_m^\dagger\hat{a}_n+\frac{\partial_\eta\Delta_{m,n}}{2}\hat{a}_m^\dagger\hat{a}_n^\dagger+\frac{\partial_\eta\Delta_{m,n}^*}{2}\hat{a}_m\hat{a}_n\right)e^{-i\hat{H}tx}\\
=&\sum_{m,n=1}^{N}-ite^{-i\hat{H}t}\int_{x=0}^{1} dx\cdot\left[\partial_\eta h_{m,n}\hat{a}_m^\dagger(xt)\hat{a}_n(xt)+\frac{\partial_\eta\Delta_{m,n}}{2}\hat{a}_m^\dagger(xt)\hat{a}_n^\dagger(xt)+\frac{\partial_\eta\Delta_{m,n}^*}{2}\hat{a}_m(xt)\hat{a}_n(xt)\right]\\
=&\sum_{m,n=1}^{N}-ie^{-i\hat{H}t}\int_{y=0}^{t} dy\cdot\left[\partial_\eta h_{m,n}\hat{a}_m^\dagger(y)\hat{a}_n(y)+\frac{\partial_\eta\Delta_{m,n}}{2}\hat{a}_m^\dagger(y)\hat{a}_n^\dagger(y)+\frac{\partial_\eta\Delta_{m,n}^*}{2}\hat{a}_m(y)\hat{a}_n(y)\right],
\end{aligned}\tag{S9}$$

where $y=xt$.

Substitute Eq. (S8) into Eq. (S9) (for convenience, we use $P_{j,k}$ and $Q_{j,k}$ to represent $P_{j,k}(y)$ and $Q_{j,k}(y)$, respectively), we have

$$\begin{aligned}
&\partial_\eta e^{-i\hat{H}t}\\
=&\sum_{m,n,j,k=1}^{N}-ie^{-i\hat{H}t}\int_{y=0}^{t} dy\cdot\Big[\partial_\eta h_{m,n}\left(P_{m,j}^*\hat{a}_j^\dagger+Q_{m,j}^*\hat{a}_j\right)\left(P_{n,k}\hat{a}_k+Q_{n,k}\hat{a}_k^\dagger\right)+\\
&\frac{\partial_\eta\Delta_{m,n}}{2}\left(P_{m,j}^*\hat{a}_j^\dagger+Q_{m,j}^*\hat{a}_j\right)\left(P_{n,k}^*\hat{a}_k^\dagger+Q_{n,k}^*\hat{a}_k\right)+\frac{\partial_\eta\Delta_{m,n}^*}{2}\left(P_{m,j}\hat{a}_j+Q_{m,j}\hat{a}_j^\dagger\right)\left(P_{n,k}\hat{a}_k+Q_{n,k}\hat{a}_k^\dagger\right)\Big]\\
=&\sum_{m,n,j,k=1}^{N}-ie^{-i\hat{H}t}\int_{y=0}^{t} dy\cdot\Big[\Big(\partial_\eta h_{m,n}P_{m,j}^*P_{n,k}+\frac{\partial_\eta\Delta_{m,n}}{2}P_{m,j}^*Q_{n,k}^*+\frac{\partial_\eta\Delta_{m,n}^*}{2}Q_{m,j}P_{n,k}\Big)\hat{a}_j^\dagger\hat{a}_k+(\partial_\eta h_{m,n}P_{m,j}^*Q_{n,k}\\
&+\frac{\partial_\eta\Delta_{m,n}}{2}P_{m,j}^*P_{n,k}^*+\frac{\partial_\eta\Delta_{m,n}^*}{2}Q_{m,j}Q_{n,k}\Big)\hat{a}_j^\dagger\hat{a}_k^\dagger+\Big(\partial_\eta h_{m,n}Q_{m,j}^*P_{n,k}+\frac{\partial_\eta\Delta_{m,n}}{2}Q_{m,j}^*Q_{n,k}^*+\frac{\partial_\eta\Delta_{m,n}^*}{2}P_{m,j}P_{n,k}\Big)\hat{a}_j\hat{a}_k\\
&+\Big(\partial_\eta h_{m,n}Q_{m,j}^*Q_{n,k}+\frac{\partial_\eta\Delta_{m,n}}{2}Q_{m,j}^*P_{n,k}^*+\frac{\partial_\eta\Delta_{m,n}^*}{2}P_{m,j}Q_{n,k}\Big)\hat{a}_j\hat{a}_k^\dagger\Big]
\end{aligned}\tag{S10}$$

$$\begin{aligned}
=&\sum_{m,n,j,k=1}^{N}-ie^{-i\hat{H}t}\int_{y=0}^{t} dy\cdot\Big[\Big(\partial_\eta h_{m,n}(P_{m,j}^*P_{n,k}+Q_{m,k}^*Q_{n,j})+\frac{\partial_\eta\Delta_{m,n}}{2}(P_{m,j}^*Q_{n,k}^*+Q_{m,k}^*P_{n,j}^*)+\\
&\frac{\partial_\eta\Delta_{m,n}^*}{2}(Q_{m,j}P_{n,k}+P_{m,k}Q_{n,j})\Big)\hat{a}_j^\dagger\hat{a}_k+\Big(\partial_\eta h_{m,n}P_{m,j}^*Q_{n,k}+\frac{\partial_\eta\Delta_{m,n}}{2}P_{m,j}^*P_{n,k}^*+\frac{\partial_\eta\Delta_{m,n}^*}{2}Q_{m,j}Q_{n,k}\Big)\hat{a}_j^\dagger\hat{a}_k^\dagger+\\
&\Big(\partial_\eta h_{m,n}Q_{m,j}^*P_{n,k}+\frac{\partial_\eta\Delta_{m,n}}{2}Q_{m,j}^*Q_{n,k}^*+\frac{\partial_\eta\Delta_{m,n}^*}{2}P_{m,j}P_{n,k}\Big)\hat{a}_j\hat{a}_k+\\
&\Big(\partial_\eta h_{m,n}Q_{m,j}^*Q_{n,k}+\frac{\partial_\eta\Delta_{m,n}}{2}Q_{m,j}^*P_{n,k}^*+\frac{\partial_\eta\Delta_{m,n}^*}{2}P_{m,j}Q_{n,k}\Big)\delta_{j,k}\Big]\\
=&-\frac{i}{2}e^{-i\hat{H}t}\left[C_0+\sum_{k,j}\left(2C_{1,k,j}\hat{a}_k^\dagger\hat{a}_j+C_{2,k,j}\hat{a}_k^\dagger\hat{a}_j^\dagger+C_{3,k,j}\hat{a}_k\hat{a}_j\right)\right]\\
=&e^{-i\hat{H}t}\hat{\mathcal{O}}.
\end{aligned}\tag{S11}$$

Here

$$
\begin{aligned}
C_0 =& \sum_{m,n,j=1}^{N} 2\int_{y=0}^{t} dy \left(\partial_\eta h_{m,n} Q^*_{m,j} Q_{n,j} + \frac{\partial_\eta \Delta_{m,n}}{2} Q^*_{m,j} P^*_{n,j} + \frac{\partial_\eta \Delta^*_{m,n}}{2} P_{m,j} Q_{n,j}\right) \\
C_{1,j,k} =& \sum_{m,n=1}^{N} \int_{y=0}^{t} dy \Bigg[\partial_\eta h_{m,n} (P^*_{m,j} P_{n,k} + Q^*_{m,k} Q_{n,j}) + \frac{\partial_\eta \Delta_{m,n}}{2} (P^*_{m,j} Q^*_{n,k} + Q^*_{m,k} P^*_{n,j}) + \\
& \frac{\partial_\eta \Delta^*_{m,n}}{2} (Q_{m,j} P_{n,k} + P_{m,k} Q_{n,j})\Bigg] \\
C_{2,j,k} =& \sum_{m,n=1}^{N} \int_{y=0}^{t} dy \Bigg[\partial_\eta h_{m,n} \left(P^*_{m,j} Q_{n,k} + P^*_{m,k} Q_{n,j}\right) + \frac{\partial_\eta \Delta_{m,n}}{2} \left(P^*_{m,j} P^*_{n,k} + P^*_{m,k} P^*_{n,j}\right) + \\
& \frac{\partial_\eta \Delta^*_{m,n}}{2} \left(Q_{m,j} Q_{n,k} + Q_{m,k} Q_{n,j}\right)\Bigg] \\
C_{3,j,k} =& \sum_{m,n=1}^{N} \int_{y=0}^{t} dy \Bigg[\partial_\eta h_{m,n} \left(Q^*_{m,j} P_{n,k} + Q^*_{m,k} P_{n,j}\right) + \frac{\partial_\eta \Delta_{m,n}}{2} \left(Q^*_{m,j} Q^*_{n,k} + Q^*_{m,k} Q^*_{n,j}\right) + \\
& \frac{\partial_\eta \Delta^*_{m,n}}{2} \left(P_{m,j} P_{n,k} + P_{m,k} P_{n,j}\right)\Bigg] \\
\hat{\mathcal{O}} =& -\frac{i}{2}\left[C_0 + \sum_{k,j}\left(2C_{1,k,j} \hat{a}^\dagger_k \hat{a}_j + C_{2,k,j} \hat{a}^\dagger_k \hat{a}^\dagger_j + C_{3,k,j} \hat{a}_k \hat{a}_j\right)\right].
\end{aligned}
\tag{S12}
$$

$\boldsymbol{C}_z$ $(z = 1, 2, 3)$, P, and Q are $N \times N$ matrices and $[\boldsymbol{C}_z]_{j_1,j_2} = C_{z,j_1,j_2}$. In the matrix form, we can rewrite the above equations as

$$
\begin{pmatrix} \boldsymbol{C}_1 & \boldsymbol{C}_2 \\ \boldsymbol{C}^*_2 & \boldsymbol{C}^*_1 \end{pmatrix} = \int_{y=0}^{t} dy [S(y)]^\dagger \Sigma_z \partial_\eta H_D S(y), \tag{S13}
$$

where $\Sigma_z = \sigma_z \otimes \mathbb{I}$, $S(y) = e^{-iyH_D}$, σ_z is a Pauli matrix, and $\mathbb{I}$ is the $N \times N$ identity matrix.

The QFI becomes

$$
F_\eta = 4[\langle\psi_0|\hat{\mathcal{O}}^\dagger \hat{\mathcal{O}}|\psi_0\rangle - |\langle\psi_0|\hat{\mathcal{O}}|\psi_0\rangle|^2]. \tag{S14}
$$

Notice that we have

$$
\hat{D}^{-1}(\alpha_j) \hat{a}_j \hat{D}(\alpha_j) = e^{-\alpha_j \hat{a}^\dagger_j + \alpha^*_j \hat{a}_j} \hat{a}_j e^{\alpha_j \hat{a}^\dagger_j - \alpha^*_j \hat{a}_j} = \hat{a}_j + \alpha_j,
$$

$$
\begin{aligned}
\hat{a}_j|\psi_0\rangle =& \hat{a}_j \hat{D}_1(\alpha_1) \hat{D}_2(\alpha_2) ... \hat{D}_j(\alpha_j) ... \hat{D}_N(\alpha_N)|0\rangle \\
=& \hat{D}_j(\alpha_j) \hat{D}_j(-\alpha_j) \hat{a}_j \hat{D}_1(\alpha_1) \hat{D}_2(\alpha_2) ... \hat{D}_j(\alpha_j) ... \hat{D}_N(\alpha_N)|0\rangle \\
=& \alpha_j|\psi_0\rangle,
\end{aligned}
\tag{S15}
$$

and

$$
\langle\psi_0|\hat{a}^\dagger_j = \alpha^*_j \langle\psi_0|. \tag{S16}
$$

Take Eq. (S12) into Eq. (S14), and we expand the first term of Eq. (S14) as a summation of normal ordered terms (NOTs). According to Eqs. (S15) and (S16), the normal ordered quadratic terms (NOQTs) of the first and second terms of Eq. (S14) cancel with each other. We have

$$\begin{aligned}
&\langle\psi_0|\hat{\mathcal{O}}^\dagger\hat{\mathcal{O}}|\psi_0\rangle\\
=&\frac{1}{4}\langle\psi_0|\left[C_0+\sum_{j_1,j_2=1}^{N}(2C^*_{1,j_2,j_1}\hat{a}^\dagger_{j_1}\hat{a}_{j_2}+C^*_{2,j_1,j_2}\hat{a}_{j_1}\hat{a}_{j_2}+C^*_{3,j_1,j_2}\hat{a}^\dagger_{j_1}\hat{a}^\dagger_{j_2})\right]\times\\
&\left[C_0+\sum_{k_1,k_2=1}^{N}(2C_{1,k_1,k_2}\hat{a}^\dagger_{k_1}\hat{a}_{k_2}+C_{2,k_1,k_2}\hat{a}^\dagger_{k_1}\hat{a}^\dagger_{k_2}+C_{3,k_1,k_2}\hat{a}_{k_1}\hat{a}_{k_2})\right]|\psi_0\rangle\\
=&\frac{1}{4}\langle\psi_0|\sum_{j_1,j_2,k_1,k_2=1}^{N}\Big(4C^*_{1,j_2,j_1}C_{1,k_1,k_2}\hat{a}^\dagger_{j_1}\hat{a}_{j_2}\hat{a}^\dagger_{k_1}\hat{a}_{k_2}+2C^*_{1,j_2,j_1}C_{2,k_1,k_2}\hat{a}^\dagger_{j_1}\hat{a}_{j_2}\hat{a}^\dagger_{k_1}\hat{a}^\dagger_{k_2}+\\
&2C^*_{2,j_1,j_2}C_{1,k_1,k_2}\hat{a}_{j_1}\hat{a}_{j_2}\hat{a}^\dagger_{k_1}\hat{a}_{k_2}+C^*_{2,j_1,j_2}C_{2,k_1,k_2}\hat{a}_{j_1}\hat{a}_{j_2}\hat{a}^\dagger_{k_1}\hat{a}^\dagger_{k_2}+NOQTs\Big)|\psi_0\rangle,
\end{aligned}\tag{S17}$$

$$\hat{a}^\dagger_{j_1}\hat{a}_{j_2}\hat{a}^\dagger_{k_1}\hat{a}_{k_2}=\hat{a}^\dagger_{j_1}\hat{a}^\dagger_{k_1}\hat{a}_{j_2}\hat{a}_{k_2}+\delta_{k_1,j_2}\hat{a}^\dagger_{j_1}\hat{a}_{k_2},\tag{S18}$$

$$\hat{a}^\dagger_{j_1}\hat{a}_{j_2}\hat{a}^\dagger_{k_1}\hat{a}^\dagger_{k_2}=\hat{a}^\dagger_{j_1}\hat{a}^\dagger_{k_1}\hat{a}_{j_2}\hat{a}^\dagger_{k_2}+\delta_{j_2,k_1}\hat{a}^\dagger_{j_1}\hat{a}^\dagger_{k_2}=\hat{a}^\dagger_{j_1}\hat{a}^\dagger_{k_1}\hat{a}^\dagger_{k_2}\hat{a}_{j_2}+\delta_{j_2,k_2}\hat{a}^\dagger_{j_1}\hat{a}^\dagger_{k_1}+\delta_{j_2,k_1}\hat{a}^\dagger_{j_1}\hat{a}^\dagger_{k_2},\tag{S19}$$

$$\hat{a}_{j_1}\hat{a}_{j_2}\hat{a}^\dagger_{k_1}\hat{a}_{k_2}=\hat{a}_{j_1}\hat{a}^\dagger_{k_1}\hat{a}_{j_2}\hat{a}_{k_2}+\delta_{k_1,j_2}\hat{a}_{j_1}\hat{a}_{k_2}=\hat{a}^\dagger_{k_1}\hat{a}_{j_1}\hat{a}_{j_2}\hat{a}_{k_2}+\delta_{j_1,k_1}\hat{a}_{j_2}\hat{a}_{k_2}+\delta_{k_1,j_2}\hat{a}_{j_1}\hat{a}_{k_2},\tag{S20}$$

and

$$\begin{aligned}
&\hat{a}_{j_1}\hat{a}_{j_2}\hat{a}^\dagger_{k_1}\hat{a}^\dagger_{k_2}\\
=&\hat{a}_{j_1}\hat{a}^\dagger_{k_1}\hat{a}_{j_2}\hat{a}^\dagger_{k_2}+\delta_{j_2,k_1}\hat{a}_{j_1}\hat{a}^\dagger_{k_2}\\
=&\hat{a}^\dagger_{k_1}\hat{a}_{j_1}\hat{a}_{j_2}\hat{a}^\dagger_{k_2}+\delta_{j_1,k_1}\hat{a}_{j_2}\hat{a}^\dagger_{k_2}+\delta_{j_2,k_1}\hat{a}_{j_1}\hat{a}^\dagger_{k_2}\\
=&\hat{a}^\dagger_{k_1}\hat{a}_{j_1}\hat{a}^\dagger_{k_2}\hat{a}_{j_2}+\delta_{k_2,j_2}\hat{a}^\dagger_{k_1}\hat{a}_{j_1}+\delta_{j_1,k_1}\hat{a}_{j_2}\hat{a}^\dagger_{k_2}+\delta_{j_2,k_1}\hat{a}_{j_1}\hat{a}^\dagger_{k_2}\\
=&\hat{a}^\dagger_{k_1}\hat{a}^\dagger_{k_2}\hat{a}_{j_1}\hat{a}_{j_2}+\delta_{j_1,k_2}\hat{a}^\dagger_{k_1}\hat{a}_{j_2}+\delta_{k_2,j_2}\hat{a}^\dagger_{k_1}\hat{a}_{j_1}+\delta_{j_1,k_1}\hat{a}_{j_2}\hat{a}^\dagger_{k_2}+\delta_{j_2,k_1}\hat{a}_{j_1}\hat{a}^\dagger_{k_2}\\
=&\hat{a}^\dagger_{k_1}\hat{a}^\dagger_{k_2}\hat{a}_{j_1}\hat{a}_{j_2}+\delta_{j_1,k_2}\hat{a}^\dagger_{k_1}\hat{a}_{j_2}+\delta_{k_2,j_2}\hat{a}^\dagger_{k_1}\hat{a}_{j_1}+\delta_{j_1,k_1}\hat{a}^\dagger_{k_2}\hat{a}_{j_2}+\delta_{j_2,k_1}\hat{a}^\dagger_{k_2}\hat{a}_{j_1}+\delta_{j_1,k_1}\delta_{j_2,k_2}+\delta_{j_2,k_1}\delta_{j_1,k_2}.
\end{aligned}\tag{S21}$$

Take Eqs. (S12) and (S17)-(S21) into Eq. (S14), we can get that

$$\begin{aligned}
F_\eta=&4[\langle\psi_0|\hat{\mathcal{O}}^\dagger\hat{\mathcal{O}}|\psi_0\rangle-|\langle\psi_0|\hat{\mathcal{O}}|\psi_0\rangle|^2]\\
=&4\Bigg\{\frac{1}{4}\langle\psi_0|\sum_{j_1,j_2,k_1,k_2=1}^{N}\Big(4C^*_{1,j_2,j_1}C_{1,k_1,k_2}\delta_{k_1,j_2}\hat{a}^\dagger_{j_1}\hat{a}_{k_2}+2C^*_{1,j_2,j_1}C_{2,k_1,k_2}(\delta_{j_2,k_2}\hat{a}^\dagger_{j_1}\hat{a}^\dagger_{k_1}+\delta_{j_2,k_1}\hat{a}^\dagger_{j_1}\hat{a}^\dagger_{k_2})+\\
&2C^*_{2,j_1,j_2}C_{1,k_1,k_2}(\delta_{j_1,k_1}\hat{a}_{j_2}\hat{a}_{k_2}+\delta_{k_1,j_2}\hat{a}_{j_1}\hat{a}_{k_2})+C^*_{2,j_1,j_2}C_{2,k_1,k_2}(\delta_{j_1,k_2}\hat{a}^\dagger_{k_1}\hat{a}_{j_2}+\delta_{k_2,j_2}\hat{a}^\dagger_{k_1}\hat{a}_{j_1}+\delta_{j_1,k_1}\hat{a}^\dagger_{k_2}\hat{a}_{j_2}+\\
&\delta_{j_2,k_1}\hat{a}^\dagger_{k_2}\hat{a}_{j_1}+\delta_{j_1,k_1}\delta_{j_2,k_2}+\delta_{j_2,k_1}\delta_{j_1,k_2})+NOQT\Big)|\psi_0\rangle-|\langle\psi_0|\hat{\mathcal{O}}|\psi_0\rangle|^2\Bigg\}\\
=&\sum_{j_1,j_2,k_1,k_2=1}^{N}\big[4C^*_{1,j_2,j_1}C_{1,k_1,k_2}\delta_{k_1,j_2}\alpha^*_{j_1}\alpha_{k_2}+2C^*_{1,j_2,j_1}C_{2,k_1,k_2}(\delta_{j_2,k_2}\alpha^*_{j_1}\alpha^*_{k_1}+\delta_{j_2,k_1}\alpha^*_{j_1}\alpha^*_{k_2})+\\
&2C^*_{2,j_1,j_2}C_{1,k_1,k_2}(\delta_{j_1,k_1}\alpha_{j_2}\alpha_{k_2}+\delta_{k_1,j_2}\alpha_{j_1}\alpha_{k_2})+C^*_{2,j_1,j_2}C_{2,k_1,k_2}(\delta_{j_1,k_2}\alpha^*_{k_1}\alpha_{j_2}+\delta_{k_2,j_2}\alpha^*_{k_1}\alpha_{j_1}+\delta_{j_1,k_1}\alpha^*_{k_2}\alpha_{j_2}+\\
&\delta_{j_2,k_1}\alpha^*_{k_2}\alpha_{j_1}+\delta_{j_1,k_1}\delta_{j_2,k_2}+\delta_{j_2,k_1}\delta_{j_1,k_2})\big]\\
=&\sum_{j_1,j_2,k_1}\big(4C^*_{1,j_2,j_1}C_{1,j_2,k_1}\alpha^*_{j_1}\alpha_{k_1}+2C^*_{1,j_2,j_1}C_{2,k_1,j_2}\alpha^*_{j_1}\alpha^*_{k_1}+2C^*_{1,j_2,j_1}C_{2,j_2,k_1}\alpha^*_{j_1}\alpha^*_{k_1}+\\
&2C^*_{2,j_1,j_2}C_{1,j_1,k_1}\alpha_{j_2}\alpha_{k_1}+2C^*_{2,j_1,j_2}C_{1,j_2,k_1}\alpha_{j_1}\alpha_{k_1}+C^*_{2,j_1,j_2}C_{2,k_1,j_1}\alpha^*_{k_1}\alpha_{j_2}+C^*_{2,j_1,j_2}C_{2,k_1,j_2}\alpha^*_{k_1}\alpha_{j_1}+\\
&C^*_{2,j_1,j_2}C_{2,j_1,k_1}\alpha^*_{k_1}\alpha_{j_2}+C^*_{2,j_1,j_2}C_{2,j_2,k_1}\alpha^*_{k_1}\alpha_{j_1}\big)+\sum_{j_1,j_2}\left(C^*_{2,j_1,j_2}C_{2,j_1,j_2}+C^*_{2,j_1,j_2}C_{2,j_2,j_1}\right).
\end{aligned}\tag{S22}$$

Notice that $C_{z,j_1,j_2} = C_{z,j_2,j_1}$ for any $z = 2,3$ and $j_1, j_2 = 1, 2, ..., N$ according to Eq. (S12), then we have

$$\begin{aligned} F_\eta = &\Bigg[\sum_{j_1,j_2,k_1} \big(4C^*_{1,j_2,j_1} C_{1,j_2,k_1} \alpha^*_{j_1} \alpha_{k_1} + 4C^*_{1,j_2,j_1} C_{2,k_1,j_2} \alpha^*_{j_1} \alpha^*_{k_1} + 4C^*_{2,j_1,j_2} C_{1,j_1,k_1} \alpha_{j_2} \alpha_{k_1} + \\ &2C^*_{2,j_1,j_2} C_{2,k_1,j_1} \alpha^*_{k_1} \alpha_{j_2} + 2C^*_{2,j_1,j_2} C_{2,j_1,k_1} \alpha^*_{k_1} \alpha_{j_2}\big) + \sum_{j_1,j_2} 2C^*_{2,j_1,j_2} C_{2,j_1,j_2}\Bigg] \\ = &\sum_{j_1,j_2}\left[\sum_{k_1} \big(4C^*_{1,j_2,j_1} C_{1,j_2,k_1} \alpha^*_{j_1} \alpha_{k_1} + 8\mathrm{Re}[C^*_{1,j_2,j_1} C_{2,k_1,j_2} \alpha^*_{j_1} \alpha^*_{k_1}] + 4C^*_{2,j_1,j_2} C_{2,j_1,k_1} \alpha^*_{k_1} \alpha_{j_2}\big) + 2|C_{2,j_1,j_2}|^2\right]. \end{aligned} \tag{S23}$$

In term of matrices, we get

$$\begin{aligned} F_\eta =& 4\boldsymbol{\alpha}^\dagger \boldsymbol{C}_1^\dagger \boldsymbol{C}_1 \boldsymbol{\alpha} + 8\mathrm{Re}[\boldsymbol{\alpha}^\dagger \boldsymbol{C}_2 \boldsymbol{C}_1^* \boldsymbol{\alpha}^*] + 4\boldsymbol{\alpha}^\mathrm{T} \boldsymbol{C}_2^\dagger \boldsymbol{C}_2 \boldsymbol{\alpha}^* + 2\mathrm{Tr}[\boldsymbol{C}_2^\dagger \boldsymbol{C}_2] \\ =& 4\boldsymbol{B}^\dagger \boldsymbol{B} + 2\mathrm{Tr}[\boldsymbol{C}_2^\dagger \boldsymbol{C}_2]. \end{aligned} \tag{S24}$$

where $\boldsymbol{B} = \boldsymbol{C}_1\boldsymbol{\alpha} + \boldsymbol{C}_2\boldsymbol{\alpha}^*$ and $\boldsymbol{\alpha} = [\alpha_1, \alpha_2, ..., \alpha_N]^\mathrm{T}$ and T is transpose operator. $\boldsymbol{C}_1$ and $\boldsymbol{C}_2$ are $N \times N$ matrices given in Eq. (S13).

B. QFI for general initial state and time-dependent Hamiltonian

Here we consider a general initial state $|\psi_0\rangle = \sum_{j=1}^{l} f_j |\psi_j\rangle$, where $\sum_{j=1}^{l} |f_j|^2 = 1$, $|\psi_j\rangle = |\alpha_1^j, \alpha_2^j, ..., \alpha_N^j\rangle$, $\boldsymbol{\alpha}^j = [\alpha_1^j, \alpha_2^j, ..., \alpha_N^j]^\mathrm{T}$, and $\boldsymbol{\alpha}^j \neq \boldsymbol{\alpha}^k$ for $j \neq k$. The time-dependent Hamiltonian

$$\hat{H}(t) = \sum_{j,k=1}^{N} (h_{j,k}(t) \hat{a}_j^\dagger \hat{a}_k + \frac{\Delta_{j,k}(t)}{2} \hat{a}_j^\dagger \hat{a}_k^\dagger + \frac{\Delta^*_{j,k}(t)}{2} \hat{a}_j \hat{a}_k). \tag{S25}$$

The QFI is

$$\begin{aligned} F_\eta =& 4[\langle\psi_0|\hat{\mathcal{O}}^\dagger \hat{\mathcal{O}}|\psi_0\rangle - |\langle\psi_0|\hat{\mathcal{O}}|\psi_0\rangle|^2] \\ =& 4[(\sum_{j=1}^{l} f_j^* \langle\psi_j|)\hat{\mathcal{O}}^\dagger \hat{\mathcal{O}}(\sum_{j=1}^{l} f_k |\psi_k\rangle) - |(\sum_{j=1}^{l} f_j^* \langle\psi_j|)\hat{\mathcal{O}}(\sum_{j=1}^{l} f_k |\psi_k\rangle)|^2] \\ =& 4[\sum_{j,k=1}^{l} f_j^* f_k \langle\psi_j|\hat{\mathcal{O}}^\dagger \hat{\mathcal{O}}|\psi_k\rangle - (\sum_{j,k=1}^{l} f_j^* f_k \langle\psi_j|\hat{\mathcal{O}}|\psi_k\rangle)(\sum_{m,n=1}^{l} f_m^* f_n \langle\psi_m|\hat{\mathcal{O}}^\dagger|\psi_n\rangle)] \\ =& 4[\sum_{j,k=1}^{l} f_j^* f_k \langle\psi_j|\hat{\mathcal{O}}^\dagger \hat{\mathcal{O}}|\psi_k\rangle - \sum_{j,k,m,n=1}^{l} f_j^* f_k f_m^* f_n \langle\psi_j|\hat{\mathcal{O}}|\psi_k\rangle \langle\psi_m|\hat{\mathcal{O}}^\dagger|\psi_n\rangle] \end{aligned} \tag{S26}$$

$$\begin{aligned} &\langle\psi_j|\hat{\mathcal{O}}|\psi_k\rangle \\ =&\langle\psi_j|\left[C_0 + \sum_{k_1,k_2=1}^{N} (2C_{1,k_1,k_2} \hat{a}_{k_1}^\dagger \hat{a}_{k_2} + C_{2,k_1,k_2} \hat{a}_{k_1}^\dagger \hat{a}_{k_2}^\dagger + C_{3,k_1,k_2} \hat{a}_{k_1} \hat{a}_{k_2})\right]|\psi_k\rangle \\ =&exp\left(-\frac{|\boldsymbol{\alpha}^j|^2 + |\boldsymbol{\alpha}^k|^2}{2} + \boldsymbol{\alpha}^{j*} \cdot \boldsymbol{\alpha}^k\right)\left[C_0 + \sum_{k_1,k_2=1}^{N} (2C_{1,k_1,k_2} \alpha_{k_1}^{j\dagger} \alpha_{k_2}^k + C_{2,k_1,k_2} \alpha_{k_1}^{j\dagger} \alpha_{k_2}^{j\dagger} + C_{3,k_1,k_2} \alpha_{k_1}^k \alpha_{k_2}^k)\right] \\ =&exp\left(-\frac{|\boldsymbol{\alpha}^j|^2 + |\boldsymbol{\alpha}^k|^2}{2} + \boldsymbol{\alpha}^{j*} \cdot \boldsymbol{\alpha}^k\right)\left[C_0 + 2\boldsymbol{\alpha}^{j\dagger} \boldsymbol{C}_1 \boldsymbol{\alpha}^k + \boldsymbol{\alpha}^{j\dagger} \boldsymbol{C}_2 \boldsymbol{\alpha}^{j*} + \boldsymbol{\alpha}^{k\mathbf{T}} \boldsymbol{C}_2^* \boldsymbol{\alpha}^k\right], \end{aligned}$$

where we use $\boldsymbol{C}_2^* = \boldsymbol{C}_3$.

$$\begin{aligned}
&\langle\psi_m|\hat{\mathcal{O}}^\dagger|\psi_n\rangle \\
=&\langle\psi_n|\hat{\mathcal{O}}|\psi_m\rangle^\dagger \\
=&exp\left(-\frac{|\boldsymbol{\alpha}^m|^2+|\boldsymbol{\alpha}^n|^2}{2}+\boldsymbol{\alpha}^n\cdot\boldsymbol{\alpha}^{m*}\right)(C_0+2\boldsymbol{\alpha}^{n\dagger}\boldsymbol{C}_1\boldsymbol{\alpha}^m+\boldsymbol{\alpha}^{n\dagger}\boldsymbol{C}_2\boldsymbol{\alpha}^{n*}+\boldsymbol{\alpha}^{m\mathbf{T}}\boldsymbol{C}_3\boldsymbol{\alpha}^m)^\dagger \\
=&exp\left(-\frac{|\boldsymbol{\alpha}^m|^2+|\boldsymbol{\alpha}^n|^2}{2}+\boldsymbol{\alpha}^n\cdot\boldsymbol{\alpha}^{m*}\right)\left[C_0+2\boldsymbol{\alpha}^{m\dagger}\boldsymbol{C}_1\boldsymbol{\alpha}^n+\boldsymbol{\alpha}^{n\mathbf{T}}\boldsymbol{C}_2^*\boldsymbol{\alpha}^n+\boldsymbol{\alpha}^{m\dagger}\boldsymbol{C}_2\boldsymbol{\alpha}^{m*}\right]
\end{aligned} \tag{S27}$$

$$\begin{aligned}
&\langle\psi_j|\hat{\mathcal{O}}^\dagger\hat{\mathcal{O}}|\psi_k\rangle \\
=&\frac{1}{4}\langle\psi_j|\left[C_0+\sum_{j_1,j_2=1}^{N}(2C^*_{1,j_2,j_1}\hat{a}^\dagger_{j_1}\hat{a}_{j_2}+C^*_{2,j_1,j_2}\hat{a}_{j_1}\hat{a}_{j_2}+C^*_{3,j_1,j_2}\hat{a}^\dagger_{j_1}\hat{a}^\dagger_{j_2})\right]\times \\
&\left[C_0+\sum_{k_1,k_2=1}^{N}(2C_{1,k_1,k_2}\hat{a}^\dagger_{k_1}\hat{a}_{k_2}+C_{2,k_1,k_2}\hat{a}^\dagger_{k_1}\hat{a}^\dagger_{k_2}+C_{3,k_1,k_2}\hat{a}_{k_1}\hat{a}_{k_2})\right]|\psi_k\rangle \\
=&\frac{1}{4}\langle\psi_j|\sum_{j_1,j_2,k_1,k_2=1}^{N}\Big(4C^*_{1,j_2,j_1}C_{1,k_1,k_2}\hat{a}^\dagger_{j_1}\hat{a}_{j_2}\hat{a}^\dagger_{k_1}\hat{a}_{k_2}+2C^*_{1,j_2,j_1}C_{2,k_1,k_2}\hat{a}^\dagger_{j_1}\hat{a}_{j_2}\hat{a}^\dagger_{k_1}\hat{a}^\dagger_{k_2}+ \\
&2C^*_{2,j_1,j_2}C_{1,k_1,k_2}\hat{a}_{j_1}\hat{a}_{j_2}\hat{a}^\dagger_{k_1}\hat{a}_{k_2}+C^*_{2,j_1,j_2}C_{2,k_1,k_2}\hat{a}_{j_1}\hat{a}_{j_2}\hat{a}^\dagger_{k_1}\hat{a}^\dagger_{k_2}+NOQTs\Big)|\psi_k\rangle.
\end{aligned} \tag{S28}$$

For $R_{j,k} = 4(\langle\psi_j|\hat{\mathcal{O}}^\dagger\hat{\mathcal{O}}|\psi_k\rangle - \langle\psi_j|\hat{\mathcal{O}}^\dagger|\psi_k\rangle\langle\psi_j|\hat{\mathcal{O}}|\psi_k\rangle/\langle\psi_j|\psi_k\rangle)$, the NOQT of the first term cancels with that of the second term. We have

$$\begin{aligned}
R_{j,k}=&4[\langle\psi_j|\hat{\mathcal{O}}^\dagger\hat{\mathcal{O}}|\psi_k\rangle-\langle\psi_j|\hat{\mathcal{O}}^\dagger|\psi_k\rangle\langle\psi_j|\hat{\mathcal{O}}|\psi_k\rangle/\langle\psi_j|\psi_k\rangle] \\
=&4\Bigg\{\frac{1}{4}\langle\psi_j|\sum_{j_1,j_2,k_1,k_2=1}^{N}\Big(4C^*_{1,j_2,j_1}C_{1,k_1,k_2}\delta_{k_1,j_2}\hat{a}^\dagger_{j_1}\hat{a}_{k_2}+2C^*_{1,j_2,j_1}C_{2,k_1,k_2}(\delta_{j_2,k_2}\hat{a}^\dagger_{j_1}\hat{a}^\dagger_{k_1}+\delta_{j_2,k_1}\hat{a}^\dagger_{j_1}\hat{a}^\dagger_{k_2})+ \\
&2C^*_{2,j_1,j_2}C_{1,k_1,k_2}(\delta_{j_1,k_1}\hat{a}_{j_2}\hat{a}_{k_2}+\delta_{k_1,j_2}\hat{a}_{j_1}\hat{a}_{k_2})+C^*_{2,j_1,j_2}C_{2,k_1,k_2}(\delta_{j_1,k_2}\hat{a}^\dagger_{k_1}\hat{a}_{j_2}+\delta_{k_2,j_2}\hat{a}^\dagger_{k_1}\hat{a}_{j_1}+\delta_{j_1,k_1}\hat{a}^\dagger_{k_2}\hat{a}_{j_2}+ \\
&\delta_{j_2,k_1}\hat{a}^\dagger_{k_2}\hat{a}^k_{j_1}+\delta_{j_1,k_1}\delta_{j_2,k_2}+\delta_{j_2,k_1}\delta_{j_1,k_2})+NOQT\Big)|\psi_k\rangle-\langle\psi_j|\hat{\mathcal{O}}^\dagger|\psi_k\rangle\langle\psi_j|\hat{\mathcal{O}}|\psi_k/\langle\psi_j|\psi_k\rangle\rangle)\Bigg\} \\
=&\sum_{j_1,j_2,k_1,k_2=1}^{N}\langle\psi_j|\psi_k\rangle\Big[4C^*_{1,j_2,j_1}C_{1,k_1,k_2}\delta_{k_1,j_2}\alpha^{j*}_{j_1}\alpha^k_{k_2}+2C^*_{1,j_2,j_1}C_{2,k_1,k_2}(\delta_{j_2,k_2}\alpha^{j*}_{j_1}\alpha^{j*}_{k_1}+\delta_{j_2,k_1}\alpha^{j*}_{j_1}\alpha^{j*}_{k_2})+ \\
&2C^*_{2,j_1,j_2}C_{1,k_1,k_2}(\delta_{j_1,k_1}\alpha^k_{j_2}\alpha^k_{k_2}+\delta_{k_1,j_2}\alpha^k_{j_1}\alpha^k_{k_2})+C^*_{2,j_1,j_2}C_{2,k_1,k_2}(\delta_{j_1,k_2}\alpha^{j*}_{k_1}\alpha^k_{j_2}+\delta_{k_2,j_2}\alpha^{j*}_{k_1}\alpha^k_{j_1}+\delta_{j_1,k_1}\alpha^{j*}_{k_2}\alpha^k_{j_2}+ \\
&\delta_{j_2,k_1}\alpha^{j*}_{k_2}\alpha^k_{j_1}+\delta_{j_1,k_1}\delta_{j_2,k_2}+\delta_{j_2,k_1}\delta_{j_1,k_2})\Big]
\end{aligned}$$

$$
\begin{aligned}
&= \sum_{j_1,j_2,k_1} \langle\psi_j|\psi_k\rangle \Big(4C^*_{1,j_2,j_1}C_{1,j_2,k_1}\alpha^{j*}_{j_1}\alpha^k_{k_1} + 2C^*_{1,j_2,j_1}C_{2,k_1,j_2}\alpha^{j*}_{j_1}\alpha^{j*}_{k_1} + 2C^*_{1,j_2,j_1}C_{2,j_2,k_1}\alpha^{j*}_{j_1}\alpha^{j*}_{k_1} + \\
&\quad 2C^*_{2,j_1,j_2}C_{1,j_1,k_1}\alpha^k_{j_2}\alpha^k_{k_1} + 2C^*_{2,j_1,j_2}C_{1,j_2,k_1}\alpha^k_{j_1}\alpha^k_{k_1} + C^*_{2,j_1,j_2}C_{2,k_1,j_1}\alpha^{j*}_{k_1}\alpha^k_{j_2} + C^*_{2,j_1,j_2}C_{2,k_1,j_2}\alpha^{j*}_{k_1}\alpha^k_{j_1} + \\
&\quad C^*_{2,j_1,j_2}C_{2,j_1,k_1}\alpha^{j*}_{k_1}\alpha^k_{j_2} + C^*_{2,j_1,j_2}C_{2,j_2,k_1}\alpha^{j*}_{k_1}\alpha^k_{j_1}\Big) + \sum_{j_1,j_2}\langle\psi_j|\psi_k\rangle\left(C^*_{2,j_1,j_2}C_{2,j_1,j_2} + C^*_{2,j_1,j_2}C_{2,j_2,j_1}\right) \\
&=\langle\psi_j|\psi_k\rangle \Bigg[\sum_{j_1,j_2,k_1}\Big(4C^*_{1,j_2,j_1}C_{1,j_2,k_1}\alpha^{j*}_{j_1}\alpha^k_{k_1} + 4C^*_{1,j_2,j_1}C_{2,k_1,j_2}\alpha^{j*}_{j_1}\alpha^{j*}_{k_1} + 4C^*_{2,j_1,j_2}C_{1,j_1,k_1}\alpha^k_{j_2}\alpha^k_{k_1} + \\
&\quad 2C^*_{2,j_1,j_2}C_{2,k_1,j_1}\alpha^{j*}_{k_1}\alpha^k_{j_2} + 2C^*_{2,j_1,j_2}C_{2,j_1,k_1}\alpha^{j*}_{k_1}\alpha^k_{j_2}\Big) + \sum_{j_1,j_2} 2C^*_{2,j_1,j_2}C_{2,j_1,j_2}\Bigg] \\
&= \sum_{j_1,j_2}\langle\psi_j|\psi_k\rangle\Bigg[\sum_{k_1} 4\Big(C^*_{1,j_2,j_1}C_{1,j_2,k_1}\alpha^{j*}_{j_1}\alpha^k_{k_1} + C^*_{1,j_2,j_1}C_{2,k_1,j_2}\alpha^{j*}_{j_1}\alpha^{j*}_{k_1} + C^*_{2,j_1,j_2}C_{1,j_1,k_1}\alpha^k_{j_2}\alpha^k_{k_1} + \\
&\quad C^{j*}_{2,j_1,j_2}C_{2,j_1,k_1}\alpha^{j*}_{k_1}\alpha^k_{j_2}\Big) + 2|C_{2,j_1,j_2}|^2\Bigg] \\
&=\langle\psi_j|\psi_k\rangle\left[4(\boldsymbol{\alpha}^{j\dagger}\boldsymbol{C}_1^\dagger\boldsymbol{C}_1\boldsymbol{\alpha}^k + \boldsymbol{\alpha}^{j\dagger}\boldsymbol{C}_2\boldsymbol{C}_1^*\boldsymbol{\alpha}^{j*} + \boldsymbol{\alpha}^{k\mathbf{T}}\boldsymbol{C}_2^*\boldsymbol{C}_1\boldsymbol{\alpha}^k + \boldsymbol{\alpha}^{k\mathrm{T}}\boldsymbol{C}_2^\dagger\boldsymbol{C}_2\boldsymbol{\alpha}^{j*}) + 2\mathrm{Tr}[\boldsymbol{C}_2^\dagger\boldsymbol{C}_2]\right].
\end{aligned}
\tag{S29}
$$

$$
\begin{aligned}
F_\eta =&4[\sum_{j,k=1}^{l} f_j^* f_k\langle\psi_j|\hat{\mathcal{O}}^\dagger\hat{\mathcal{O}}|\psi_k\rangle - \sum_{j,k,m,n=1}^{l} f_j^* f_k f_m^* f_n\langle\psi_j|\hat{\mathcal{O}}|\psi_k\rangle\langle\psi_m|\hat{\mathcal{O}}^\dagger|\psi_n\rangle] \\
=& \sum_{j,k=1}^{l} f_j^* f_k(R_{j,k} + 4\langle\psi_j|\hat{\mathcal{O}}^\dagger|\psi_k\rangle\langle\psi_j|\hat{\mathcal{O}}|\psi_k\rangle/\langle\psi_j|\psi_k\rangle) - \sum_{j,k,m,n=1}^{l} 4f_j^* f_k f_m^* f_n\langle\psi_j|\hat{\mathcal{O}}|\psi_k\rangle\langle\psi_m|\hat{\mathcal{O}}^\dagger|\psi_n\rangle,
\end{aligned}
\tag{S30}
$$

where $\langle\psi_j|\hat{\mathcal{O}}|\psi_k\rangle, \langle\psi_m|\hat{\mathcal{O}}^\dagger|\psi_n\rangle$, $R_{j,k}$ are given by Eqs. (S27), (S28), and (S29). $\langle\psi_j|\psi_k\rangle = exp\left(-\frac{|\boldsymbol{\alpha}^j|^2+|\boldsymbol{\alpha}^k|^2}{2} + \boldsymbol{\alpha}^{j*}\cdot\boldsymbol{\alpha}^k\right)$.

$$
\begin{aligned}
F_\eta = &\sum_{j,k=1}^{l} f_j^* f_k\langle\psi_j|\psi_k\rangle\Big\{\Big(\Big[4(\boldsymbol{\alpha}^{j\dagger}\boldsymbol{C}_1^\dagger\boldsymbol{C}_1\boldsymbol{\alpha}^k + \boldsymbol{\alpha}^{j\dagger}\boldsymbol{C}_2\boldsymbol{C}_1^*\boldsymbol{\alpha}^{j*} + \boldsymbol{\alpha}^{k\mathbf{T}}\boldsymbol{C}_2^*\boldsymbol{C}_1\boldsymbol{\alpha}^k + \boldsymbol{\alpha}^{k\mathrm{T}}\boldsymbol{C}_2^\dagger\boldsymbol{C}_2\boldsymbol{\alpha}^{j*}) + 2\mathrm{Tr}[\boldsymbol{C}_2^\dagger\boldsymbol{C}_2]\Big] + \\
&4\left(C_0 + 2\boldsymbol{\alpha}^{j\dagger}\boldsymbol{C}_1\boldsymbol{\alpha}^k + \boldsymbol{\alpha}^{j\dagger}\boldsymbol{C}_2\boldsymbol{\alpha}^{j*} + \boldsymbol{\alpha}^{k\mathbf{T}}\boldsymbol{C}_2^*\boldsymbol{\alpha}^k\right)\left(C_0 + 2\boldsymbol{\alpha}^{j\dagger}\boldsymbol{C}_1\boldsymbol{\alpha}^k + \boldsymbol{\alpha}^{k\mathbf{T}}\boldsymbol{C}_2^*\boldsymbol{\alpha}^k + \boldsymbol{\alpha}^{j\dagger}\boldsymbol{C}_2\boldsymbol{\alpha}^{j*}\right)\Big\} - \\
&\sum_{j,k,m,n=1}^{l} 4f_j^* f_k f_m^* f_n\langle\psi_j|\psi_k\rangle\langle\psi_m|\psi_n\rangle\left(C_0 + 2\boldsymbol{\alpha}^{j\dagger}\boldsymbol{C}_1\boldsymbol{\alpha}^k + \boldsymbol{\alpha}^{j\dagger}\boldsymbol{C}_2\boldsymbol{\alpha}^{j*} + \boldsymbol{\alpha}^{k\mathbf{T}}\boldsymbol{C}_2^*\boldsymbol{\alpha}^k\right)\times \\
&\left(C_0 + 2\boldsymbol{\alpha}^{m\dagger}\boldsymbol{C}_1\boldsymbol{\alpha}^n + \boldsymbol{\alpha}^{n\mathbf{T}}\boldsymbol{C}_2^*\boldsymbol{\alpha}^n + \boldsymbol{\alpha}^{m\dagger}\boldsymbol{C}_2\boldsymbol{\alpha}^{m*}\right)
\end{aligned}
\tag{S31}
$$

Finally, consider an integral initial state $|\psi_0\rangle = \int_{-\infty}^{\infty} dx f_x|\psi_x\rangle$, where $\int_{-\infty}^{\infty} dx|f_x|^2 = 1$, $|\psi_x\rangle = |\alpha_1^x, \alpha_2^x, ..., \alpha_N^x\rangle$, $\boldsymbol{\alpha}^x = [\alpha_1^x, \alpha_2^x, ..., \alpha_N^x]^{\mathrm{T}}$, and $\boldsymbol{\alpha}^x \neq \boldsymbol{\alpha}^z$ for $x \neq z$. The QFI is

$$
\begin{aligned}
F_\eta = &\int_{-\infty}^{\infty}\int_{-\infty}^{\infty} dxdz f_x^* f_z\langle\psi_x|\psi_z\rangle\Big\{\Big[4(\boldsymbol{\alpha}^{x\dagger}\boldsymbol{C}_1^\dagger\boldsymbol{C}_1\boldsymbol{\alpha}^z + \boldsymbol{\alpha}^{x\dagger}\boldsymbol{C}_2\boldsymbol{C}_1^*\boldsymbol{\alpha}^{x*} + \boldsymbol{\alpha}^{z\mathbf{T}}\boldsymbol{C}_2^*\boldsymbol{C}_1\boldsymbol{\alpha}^z + \boldsymbol{\alpha}^{z\mathrm{T}}\boldsymbol{C}_2^\dagger\boldsymbol{C}_2\boldsymbol{\alpha}^{x*}) + \\
&2\mathrm{Tr}[\boldsymbol{C}_2^\dagger\boldsymbol{C}_2]\Big] + 4\left(C_0 + 2\boldsymbol{\alpha}^{x\dagger}\boldsymbol{C}_1\boldsymbol{\alpha}^z + \boldsymbol{\alpha}^{x\dagger}\boldsymbol{C}_2\boldsymbol{\alpha}^{x*} + \boldsymbol{\alpha}^{z\mathbf{T}}\boldsymbol{C}_2^*\boldsymbol{\alpha}^z\right)\left(C_0 + 2\boldsymbol{\alpha}^{x\dagger}\boldsymbol{C}_1\boldsymbol{\alpha}^z + \boldsymbol{\alpha}^{z\mathbf{T}}\boldsymbol{C}_2^*\boldsymbol{\alpha}^z + \boldsymbol{\alpha}^{x\dagger}\boldsymbol{C}_2\boldsymbol{\alpha}^{x*}\right)\Big\} - \\
&\int_{-\infty}^{\infty}\int_{-\infty}^{\infty}\int_{-\infty}^{\infty}\int_{-\infty}^{\infty} dxdzdyds 4f_x^* f_z f_y^* f_s\langle\psi_x|\psi_z\rangle\langle\psi_y|\psi_s\rangle\left(C_0 + 2\boldsymbol{\alpha}^{x\dagger}\boldsymbol{C}_1\boldsymbol{\alpha}^z + \boldsymbol{\alpha}^{x\dagger}\boldsymbol{C}_2\boldsymbol{\alpha}^{x*} + \boldsymbol{\alpha}^{z\mathbf{T}}\boldsymbol{C}_2^*\boldsymbol{\alpha}^z\right)\times \\
&\left(C_0 + 2\boldsymbol{\alpha}^{y\dagger}\boldsymbol{C}_1\boldsymbol{\alpha}^s + \boldsymbol{\alpha}^{s\mathbf{T}}\boldsymbol{C}_2^*\boldsymbol{\alpha}^s + \boldsymbol{\alpha}^{y\dagger}\boldsymbol{C}_2\boldsymbol{\alpha}^{y*}\right).
\end{aligned}
\tag{S32}
$$

SII. QFI AND EXCEPTIONAL POINT SENSITIVITY OF A SINGLE MODE SENSOR

Consider a single mode Hamiltonian

$$\hat{H}_1 = \delta \hat{a}^\dagger \hat{a} + i\frac{\kappa}{2}(\hat{a}^{\dagger 2} - \hat{a}^2), \tag{S33}$$

with the HEOM

$$\frac{d\hat{a}}{dt} = i[\hat{H}_1, \hat{a}] = -i\delta a + \kappa a^\dagger. \tag{S34}$$

In the matrix form, we have

$$i\frac{d}{dt}\hat{V} = H_{D1}\hat{V}, \tag{S35}$$

where $\hat{V} = \left(\hat{a}, \hat{a}^\dagger\right)^T$, and $H_{D1} = \delta\tau_z + i\kappa\tau_x$ is the dynamical matrix. The EP is at $|\kappa| = |\delta|$.

$\hat{V}(t) = e^{-iH_{D1}t}\hat{V}(0) = S\hat{V}(0)$ with

$$S = e^{-iH_{D1}t} = \begin{pmatrix} P(t) & Q(t) \\ Q(t) & P^*(t) \end{pmatrix}, \tag{S36}$$

where $P(t)$ and $Q(t)$ are given by Table (S1).

TABLE S1. The values of $P(t)$ and $Q(t)$.

	$P(t)$	$Q(t)$
$\|\kappa\| > \|\delta\|$	$\cosh(\lambda_0 t) - \frac{i\delta}{\lambda_0}\sinh(\lambda_0 t)$	$\frac{\kappa}{\lambda_0}\sinh(\lambda_0 t)$
$\|\kappa\| < \|\delta\|$	$\cos(\lambda_0 t) - \frac{i\delta}{\lambda_0}\sin(\lambda_0 t)$	$\frac{\kappa}{\lambda_0}\sin(\lambda_0 t)$
$\|\kappa\| = \|\delta\|$	$1 - it\delta$	$t\delta$

For an initial state $|\psi_0\rangle = |\alpha\rangle = e^{\alpha\hat{a}^\dagger - \alpha^*\hat{a}}|0\rangle$, $|\psi_t\rangle = e^{-i\hat{H}_1 t}|\psi_0\rangle$, we have

$$\begin{aligned} F_\kappa &= 4[\langle\partial_\kappa\psi_t||\partial_\kappa\psi_t\rangle - |\langle\psi_t||\partial_\kappa\psi_t\rangle|^2] \\ &= 4|C_1\alpha + C_2\alpha^*|^2 + 2|C_2|^2, \end{aligned} \tag{S37}$$

where

$$\begin{aligned} C_1 =& i\int_{y=0}^{t} dy\,(P^*Q^* - PQ) \\ C_2 =& i\int_{y=0}^{t} dy\,\left(P^{*2} - Q^2\right). \end{aligned} \tag{S38}$$

Take Table (S1) into Eq. (S38), we get the values of C_1 and C_2 in Table (S2).

TABLE S2. The values of C_1 and C_2.

	C_1	C_2
$\|\kappa\| > \|\delta\|$	$-\frac{\delta\kappa t}{\lambda_0^2}\left[\frac{\sinh(2\lambda_0 t)}{2\lambda_0 t} - 1\right]$	$\frac{2\delta^2 t - i\delta}{2\lambda_0^2} - \frac{\kappa^2}{2\lambda_0^3}\sinh(2\lambda_0 t) + \frac{i\delta}{2\lambda_0^2}\cosh(2\lambda_0 t)$
$\|\kappa\| < \|\delta\|$	$-\frac{\delta\kappa t}{\lambda_0^2}\left[1 - \frac{\sin(2\lambda_0 t)}{2\lambda_0 t}\right]$	$\frac{i\delta - 2\kappa^2 t}{2\lambda_0^2} + \frac{\delta^2}{2\lambda_0^3}\sin(2\lambda_0 t) - \frac{i\delta}{2\lambda_0^2}\cos(2\lambda_0 t)$
$\|\kappa\| = \|\delta\|$	$-\frac{2\delta^2 t^3}{3}$	$it - \frac{2it^3\delta^2}{3} + \delta^2 t^2$

According to Eq. (S37) and Table (S2), the QFI is finite (without divergence) and continuous at or around the exceptional point (EP). Figure S1 shows QFI versus λ_0. We see QFI reaches it's maximum at EP, and decreases to

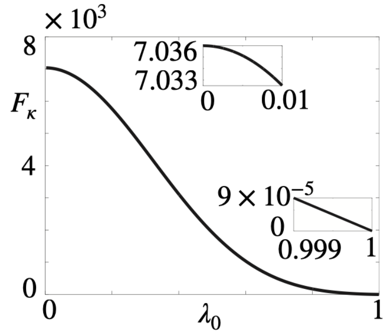

FIG. S1. QFI as a function of λ_0 for different λ_0 ranges. The parameters are $\delta = 1$ and $t = \pi$. Top inset is a quadratic function and bottom inset is a linear function.

zero when λ_0 increases to 1. $F_\kappa \propto t^6$ when $t \to +\infty$ at the EP. $F_\kappa \propto t^2$ when $t \to +\infty$ for $|\delta| > |\kappa|$. $|\delta| < |\kappa|$ is an unstable region. The $t^2 \to t^6$ time scaling demonstrates that EP does enhance the sensitivity, but it is still finite.

At EP $|\kappa| = |\delta|$, The eigenvalues of H_{D1} are

$$\omega_\pm(0) = 0. \tag{S39}$$

Adding a perturbation to κ, i.e., $\kappa = \delta - \epsilon$ ($\epsilon \ll \delta$), the eigenvalues of H_{D1} become $\omega_\pm(\epsilon)$. The eigenvalue responses are $\Delta\omega_\pm = \omega_\pm(\epsilon) - \omega_\pm(0)$. The leading orders of $\Delta\omega_\pm$ are

$$\Delta\omega_+ = (2\kappa\epsilon)^{1/2}, \quad \Delta\omega_- = -(2\kappa\epsilon)^{1/2}, \tag{S40}$$

which show a $\epsilon^{1/2}$ scaling. The $\epsilon^{1/2}$ scaling of spectrum response of the dynamical matrix corresponds to the t^6 scaling of QFI. It satisfies $d_F = 4M - 2$ and $d_\omega = 1/M$, where M is the order of EP, d_F is the scaling exponent of the QFI (i.e., $F \propto t^{d_F}$ for $t \to \infty$) and d_ω is the scaling exponent of the maximum spectrum response of the dynamical matrix [i.e., $\Delta\omega = \max_\pm(|\Delta\omega_\pm|) \propto \epsilon^{d_\omega}$ for $\epsilon \to 0$]. d_F reaches the maximum response exponent predicted by the scaling law.

SIII. QFI AND EXCEPTIONAL POINT SENSITIVITY OF A THREE MODE SENSOR

A. Without constraint

Consider a three mode Hamiltonian

$$\hat{H}_3 = i\delta(\hat{a}_1^\dagger \hat{a}_2 - \hat{a}_2^\dagger \hat{a}_1 + \hat{a}_2^\dagger \hat{a}_3 - \hat{a}_3^\dagger \hat{a}_2) + \frac{i\kappa_1}{2}(\hat{a}_1^2 - \hat{a}_1^{\dagger 2}) + \frac{i\kappa_3}{2}(\hat{a}_3^{\dagger 2} - \hat{a}_3^2). \tag{S41}$$

The HEOM is

$$i\frac{d}{dt}\hat{V}_3 = H_{D3}\hat{V}_3, \tag{S42}$$

where $\hat{V}_3 = \left(\hat{a}_1, \hat{a}_2, \hat{a}_3, \hat{a}_1^\dagger, \hat{a}_2^\dagger, \hat{a}_3^\dagger\right)^T$. $H_{D3} = \tau_0 \otimes \mathbf{K}_1 + \tau_x \otimes \mathbf{K}_2$ is the dynamical matrix, where

$$\mathbf{K}_1 = i\begin{pmatrix} 0 & \delta & 0 \\ -\delta & 0 & \delta \\ 0 & -\delta & 0 \end{pmatrix}, \mathbf{K}_2 = i\begin{pmatrix} -\kappa_1 & 0 & 0 \\ 0 & 0 & 0 \\ 0 & 0 & \kappa_3 \end{pmatrix}. \tag{S43}$$

$\hat{V}_3(t) = e^{-iH_{D3}t}\hat{V}_3(0) = S\hat{V}_3(0)$, where $S = \tau_0 \otimes P(t) + \tau_x \otimes Q(t)$.

Under a unitary transformation $(\tau_x, \tau_y, \tau_z) \to (\tau_z, \tau_y, -\tau_x)$, H_{D3} can be block diagonalized as $\tau_0 \otimes \mathbf{K}_1 + \tau_z \otimes \mathbf{K}_2$, with $H_{D3+} = \mathbf{K}_1 + \mathbf{K}_2$ and $H_{D3-} = \mathbf{K}_1 - \mathbf{K}_2$ being two irreducible blocks of H_{D3}. H_{D3+} can be regarded as the quantum generalization of the gain/neutral/loss cavity mode [9]. $H_{D3\pm}$ satisfies the parity time symmetry ($\mathcal{PT}H_{D3\pm}\mathcal{T}^{-1}\mathcal{P}^{-1} = H_{D3\pm}$) given by

$$\mathcal{P} = \begin{pmatrix} 0 & 0 & 1 \\ 0 & 1 & 0 \\ 1 & 0 & 0 \end{pmatrix} \tag{S44}$$

and $\mathcal{T}=\mathcal{K}$ is complex conjugate operator.

H_{D3} possesses two degenerate third-order EP at $\sqrt{2}\delta=\kappa_1=\kappa_3$, with the eigenvalues

$$\omega_j^{\pm}(0)=0, \qquad \text{where} \qquad j=1,2,3. \tag{S45}$$

Adding a perturbation to κ_1, i.e., $\kappa_1=\sqrt{2}\delta+\epsilon$ and $\kappa_3=\sqrt{2}\delta$ ($\epsilon\ll\delta$), the spectrum responses are $\Delta\omega_j^{\pm}=\omega_j^{\pm}(\epsilon)-\omega_j^{\pm}(0)$. Using Newton-Puiseux series expansion, the leading orders of $\Delta\omega_j^{\pm}$ are

$$\Delta\omega_j^{\pm}=ie^{i\pi j/3}\delta^{2/3}\epsilon^{1/3}, \tag{S46}$$

which have a $\epsilon^{1/3}$ scaling.

Consider the initial state $|\psi_0\rangle=|\alpha_1,\alpha_2,\alpha_3\rangle=D_1(\alpha_1)D_2(\alpha_2)D_3(\alpha_3)|0\rangle$ and $|\psi_t\rangle=e^{-i\hat{H}_3t}|\psi_0\rangle$. At the EP

$$P(t)=\begin{pmatrix} \frac{\delta^2t^2}{2}+1 & \delta t & \frac{\delta^2t^2}{2} \\ \delta(-t) & 1-\delta^2t^2 & \delta t \\ \frac{\delta^2t^2}{2} & \delta(-t) & \frac{\delta^2t^2}{2}+1 \end{pmatrix}, Q(t)=\begin{pmatrix} -\sqrt{2}\delta t & -\frac{\delta^2t^2}{\sqrt{2}} & 0 \\ \frac{\delta^2t^2}{\sqrt{2}} & 0 & \frac{\delta^2t^2}{\sqrt{2}} \\ 0 & -\frac{\delta^2t^2}{\sqrt{2}} & \sqrt{2}\delta t \end{pmatrix}. \tag{S47}$$

Take Eqs. (S47) and (S12) into Eq. (S24), we find $F_{\kappa_1}\propto t^{10}$ when $t\to+\infty$ at the third-order EP. The $\epsilon^{1/3}$ scaling of the spectrum response of the dynamical matrix corresponds to t^{10} scaling of the QFI. They also satisfy $d_F=4/d_\omega-2$.

Far from the EP at $\kappa_1=\kappa_3=0$, we have

$$P(t)=\begin{pmatrix} \cos^2\left(\frac{\delta t}{\sqrt{2}}\right) & \frac{\sin\left(\sqrt{2}\delta t\right)}{\sqrt{2}} & \sin^2\left(\frac{\delta t}{\sqrt{2}}\right) \\ -\frac{\sin\left(\sqrt{2}\delta t\right)}{\sqrt{2}} & \cos\left(\sqrt{2}\delta t\right) & \frac{\sin\left(\sqrt{2}\delta t\right)}{\sqrt{2}} \\ \sin^2\left(\frac{\delta t}{\sqrt{2}}\right) & -\frac{\sin\left(\sqrt{2}\delta t\right)}{\sqrt{2}} & \cos^2\left(\frac{\delta t}{\sqrt{2}}\right) \end{pmatrix}, Q(t)=\begin{pmatrix} 0 & 0 & 0 \\ 0 & 0 & 0 \\ 0 & 0 & 0 \end{pmatrix}. \tag{S48}$$

Take Eqs. (S48) and (S12) into Eq. (S24), we get that $F_{\kappa_1}\propto t^2$ when $t\to+\infty$ at $\kappa_1=\kappa_3=0$.

B. With constraint

Consider the same three mode model in Eq. (S41) but with the constraint $\kappa_1=\kappa_2=\eta$. The Hamiltonian becomes

$$\hat{H}_3'=i\delta(\hat{a}_1^\dagger\hat{a}_2-\hat{a}_2^\dagger\hat{a}_1+\hat{a}_2^\dagger\hat{a}_3-\hat{a}_3^\dagger\hat{a}_2)+\frac{i\eta}{2}(\hat{a}_1^2-\hat{a}_1^{\dagger 2}+\hat{a}_3^{\dagger 2}-\hat{a}_3^2), \tag{S49}$$

with the HEOM

$$i\frac{d}{dt}\hat{V}_3=H_{D3}'\hat{V}_3, \tag{S50}$$

where $\hat{V}_3=\left(\hat{a}_1,\hat{a}_2,\hat{a}_3,\hat{a}_1^\dagger,\hat{a}_2^\dagger,\hat{a}_3^\dagger\right)^T$. The dynamical matrix $H_{D3}'=\tau_0\otimes\mathbf{K}_1+\tau_x\otimes\mathbf{K}_2$ with

$$\mathbf{K}_1=i\begin{pmatrix} 0 & \delta & 0 \\ -\delta & 0 & \delta \\ 0 & -\delta & 0 \end{pmatrix}, \mathbf{K}_2=i\begin{pmatrix} -\eta & 0 & 0 \\ 0 & 0 & 0 \\ 0 & 0 & \eta \end{pmatrix}. \tag{S51}$$

$\hat{V}_3(t)=e^{-iH_{D3}'t}\hat{V}_3(0)=S\hat{V}_3(0)$, where $S=\tau_0\otimes P(t)+\tau_x\otimes Q(t)$. Add a perturbation to η, i.e., $\eta=\sqrt{2}\delta+\epsilon$ ($\epsilon\ll\delta$), and use Newton-Puiseux series expansion, we find the leading orders of the spectrum responses $\Delta\omega_j^{\pm}$ are

$$\Delta\omega_1^{\pm}=0, \quad \Delta\omega_2^{\pm}=i\sqrt{2\sqrt{2}\delta\epsilon}, \quad \Delta\omega_3^{\pm}=-i\sqrt{2\sqrt{2}\delta\epsilon}, \tag{S52}$$

which show a $\epsilon^{1/2}$ scaling for the maximum spectrum response.

We consider the initial state $|\psi_0\rangle=|0\rangle$. $|\psi_t\rangle=e^{-i\hat{H}_3't}|\psi_0\rangle$. At the third-order EP $\sqrt{2}\delta=\eta$, we have Eq. (S47). Take Eqs. (S47) and (S12) into Eq. (S24), we get that $F_\eta\propto t^6$ when $t\to+\infty$ at the third-order EP. It satisfies $d_F<4M-2$.

SIV. QFI SCALING OF BOSONIC KITAEV CHAIN

A. At exceptional point

Consider a Hamiltonian $\hat{H}_K = \hat{H}_{BKC} + \hat{H}_\eta$, where $\hat{H}_{BCK}$ is the bosonic Kitaev chain with

$$\hat{H}_{BKC} = \sum_{j=1}^{N-1} \left(iJ\hat{a}_j^\dagger \hat{a}_{j+1} + i\Omega \hat{a}_j^\dagger \hat{a}_{j+1}^\dagger + h.c. \right), \tag{S53}$$

and

$$\hat{H}_\eta = i\eta \sin(\theta)\hat{a}_N^\dagger \hat{a}_1 + i\eta\cos(\theta)\hat{a}_N^\dagger \hat{a}_1^\dagger + h.c.. \tag{S54}$$

is the edge coupling term that couples modes 1 and N. The HEOM

$$i\frac{d}{dt}\hat{V}_K = H_{DK}\hat{V}_K, \tag{S55}$$

with $\hat{V}_K = \left(\hat{a}_1, \hat{a}_2, ..., \hat{a}_N, \hat{a}_1^\dagger, \hat{a}_2^\dagger, ..., \hat{a}_N^\dagger\right)^T$, and the dynamical matrix $H_{DK} = \tau_0 \otimes \mathbf{L}_1 + \tau_x \otimes \mathbf{L}_2$. Here $\mathbf{L}_1$ and $\mathbf{L}_2$ are $N \times N$ matrices. $(\mathbf{L}_1)_{N,1} = -(\mathbf{L}_1)_{1,N} = i\eta\sin(\theta)$, $(\mathbf{L}_2)_{N,1} = (\mathbf{L}_2)_{1,N} = i\eta\cos(\theta)$, $(\mathbf{L}_1)_{j,j+1} = -(\mathbf{L}_1)_{j+1,j} = iJ$, and $(\mathbf{L}_2)_{j,j+1} = (\mathbf{L}_2)_{j+1,j} = i\Omega$, where $j = 1, 2, ..., N-1$. $\theta \in [0, 2\pi)$. Other elements of $\mathbf{L}_1$ and $\mathbf{L}_2$ are 0. Under unitary transformation $U = e^{-i\frac{\pi}{4}\tau_y}$, $(\tau_x, \tau_y, \tau_z) \to (\tau_z, \tau_y, -\tau_x)$, and H_{DK} can be block diagonalized as $\tau_0 \otimes \mathbf{L}_1 + \tau_z \otimes \mathbf{L}_2$, with $H_{DK+} = \mathbf{L}_1 + \mathbf{L}_2$ and $H_{DK-} = \mathbf{L}_1 - \mathbf{L}_2$ being two irreducible blocks of H_{DK}.

The eigenvalues of H_{DK} at the N-th order EP $J = \Omega$, $\eta = 0$ are

$$\omega_1(0) = \omega_2(0) = ... = \omega_{2N}(0) = 0. \tag{S56}$$

Add a perturbation to η, i.e., $\eta = \epsilon$ ($\epsilon \ll \Omega$), the eigenvalues of H_{DK} are denoted as $\omega_1(\epsilon)$, $\omega_2(\epsilon)$, ... $\omega_{2N}(\epsilon)$. The spectrum response are $\Delta\omega_j = \omega_j(\epsilon) - \omega_j(0)$, where $j = 1, 2, ..., 2N$. From the equation $H_{DK+}\psi = E\Psi$, where $\Psi = [\psi_1, \psi_2, ..., \psi_N]^T$, we find

$$-iE\psi_j = 2\Omega\psi_{j+1}, for \quad j = 2, 3, ..., N-1, \tag{S57}$$

$$-iE\psi_1 = \epsilon[-\sin(\theta) + \cos(\theta)]\psi_N + \epsilon[\sin(\theta) + \cos(\theta)]\psi_2, \tag{S58}$$

$$-iE\psi_N = \epsilon[-\sin(\theta) + \cos(\theta)]\psi_{N-1} + \epsilon[\sin(\theta) + \cos(\theta)]\psi_1. \tag{S59}$$

Combine Eqs. (S57)-(S59) with $\psi_1 = 1$ (we can always have that by fixing the gauge by dividing a constant for the eigenstates), we have

$$(2\Omega)^2 z^N - \epsilon^2\cos(2\theta)z^{N-2} - 2\epsilon\Omega[\cos(\theta) + \sin(\theta)] = 0, \quad z = \frac{-iE}{2\Omega}. \tag{S60}$$

For $\theta \neq \frac{3\pi}{4}$ and $\frac{7\pi}{4}$, we can omit the second term in Eq. (S60), and the maximum spectrum response has a $\epsilon^{1/N}$ scaling. Similar scaling also occurs for H_{DK-}.

Consider an initial vacuum state $|\psi_0\rangle = |0\rangle$ and $|\psi_t\rangle = e^{-i\hat{H}_K t}|\psi_0\rangle$. At the N-th order EP $J = \Omega$ and $\eta = 0$, we have

$$P(t) = \mathbb{I} + \sum_{p=1}^{N-1} \frac{(2\Omega t)^p (J_+^p + J_-^p)}{2(p!)}, Q(t) = \sum_{p=1}^{N-1} \frac{(2\Omega t)^p (J_+^p - J_-^p)}{2(p!)},$$

where $\mathbf{J}_+^p$ and $\mathbf{J}_-^p$ are $N \times N$ matrices. $(\mathbf{J}_+^p)_{j,j+p} = 1$, and $(\mathbf{J}_-^p)_{j+p,j} = (-1)^p$, where $j = 1, 2, ..., N-p$. Other elements of $\mathbf{J}_+^p$ and $\mathbf{J}_-^p$ are zero. Thus

$$\begin{aligned} [P(t)]_{j_1,j_2} =& (-1)^{(j_1-j_2)\mathrm{H}(j_1-j_2)} \frac{(2\Omega t)^{|j_1-j_2|}}{2[|j_1-j_2|!]} \quad for \quad j_1 \neq j_2, \qquad [P(t)]_{j_1,j_1} = 1 \\ [Q(t)]_{j_1,j_2} =& (-1)^{(j_1-j_2)\mathrm{H}(j_1-j_2)} \mathrm{sgn}(j_2-j_1) \frac{(2\Omega t)^{|j_1-j_2|}}{2[|j_1-j_2|!]} \quad for \quad j_1 \neq j_2, \qquad [Q(t)]_{j_1,j_1} = 0. \end{aligned} \tag{S61}$$

Here H(x) is Heaviside step function. Taking Eqs. (S61), (S12), and (S13) into Eq. (S24), we get that $F_\eta = \sum_{j,k=1}^{N} |C_{2,j,k}|^2$, where

$$\begin{aligned}
C_{2,1,N} = C_{2,N,1} &= -\frac{i}{2}\left[\cos(\theta)t + [\cos(\theta)+\sin(\theta)]\frac{2(-1)^{N-1}(2\Omega)^{2(N-1)}}{(p!)^2}t^{2N-1}\right] \\
C_{2,j,k} &= -i[\cos(\theta)+\sin(\theta)]\left[\frac{(-1)^{N-j}(2\Omega)^{N-j+k-1}t^{N-j+k}}{(N-j)!(k-1)!(N-j+k)} + \frac{(-1)^{N-k}(2\Omega)^{N-k+j-1}t^{N-k+j}}{(N-k)!(j-1)!(N-k+j)}\right], \\
C_{2,1,k} = C_{2,k,1} &= -\frac{i}{2}[\cos(\theta)+\sin(\theta)]\left[\frac{2(-1)^{N-1}(2\Omega)^{N+k-2}t^{N+k-1}}{(N-1)!(k-1)!(N+k-1)} + \frac{(-1)^{N-k}(2\Omega)^{N-k}t^{N-k+1}}{(N-k)!(N-k+1)}\right], \\
C_{2,N,k} = C_{2,k,N} &= -\frac{i}{2}[\cos(\theta)+\sin(\theta)]\left[\frac{2(-1)^{N-k}(2\Omega)^{2N-k-1}t^{2N-k}}{(N-k)!(N-1)!(2N-k)} + \frac{(2\Omega)^{k-1}t^{k}}{(k-1)!k}\right], \\
C_{2,1,1} &= -i[\cos(\theta)+\sin(\theta)]\frac{(2\Omega)^{N-1}t^{N}}{(N-1)!N} \\
C_{2,N,N} &= -i[\cos(\theta)+\sin(\theta)]\frac{(-2\Omega)^{N-1}t^{N}}{(N-1)!N},
\end{aligned} \tag{S62}$$

$j,k = 2,3,...,N-1$. When $t \to +\infty$ at the N-th order EP, $F_\eta \propto t^{4N-2}$ for $\theta \neq \frac{3\pi}{4}$ and $\frac{7\pi}{4}$, and $F_\eta \propto t^2$ for $\theta = \frac{3\pi}{4}$ or $\frac{7\pi}{4}$. The scaling exponent satisfies $d_F = 4M-2$ with $M = N$ here.

B. Region close to the exceptional point

In this section, we derive the size (N) scaling of the QFI F_η at $|J-\Omega|/|J+\Omega| \ll 1$ and $\eta = 0$ region, which is close to the EP. Under the unitary matrix $U = e^{-i\frac{\pi}{4}\tau_y}$ for the block diagonalization of $\hat{H}_{DK}$,

$$\begin{aligned}
U^\dagger H_{DK} U =& \tau_0 \otimes \mathbf{L}_1 + \tau_z \otimes \mathbf{L}_2 \\
=& \mathrm{diag}[\mathbf{L}_1 + \mathbf{L}_2, \mathbf{L}_1 - \mathbf{L}_2] \\
=& \mathrm{diag}[-\tilde{J}S^{-1}\Sigma_y S, -\tilde{J}S\Sigma_y S^{-1}],
\end{aligned} \tag{S63}$$

where $\tilde{J} = \sqrt{(J-\Omega)(J+\Omega)}$, $S = diag[1, \beta, \beta^2, ..., \beta^{N-1}]$, and $\beta = \sqrt{\frac{J+\Omega}{J-\Omega}}$. Σ_y is a $N \times N$ matrix with $[\Sigma_y]_{j,j+1} = -[\Sigma_y]_{j+1,j} = i$, and other elements being 0. Thus

$$e^{-iH_{DK}t} = U\mathrm{diag}[S^{-1}e^{i\tilde{J}\Sigma_y t}S, Se^{i\tilde{J}\Sigma_y t}S^{-1}]U^\dagger.$$

Denote $\tilde{S} = e^{i\tilde{J}\Sigma_y t}$, then we have $[S^{-1}e^{i\tilde{J}\Sigma_y t}S]_{m,n} = \tilde{S}_{m,n}\beta^{-m+n}$, $[Se^{i\tilde{J}\Sigma_y t}S^{-1}]_{m,n} = \tilde{S}_{m,n}\beta^{m-n}$, and

$$P_{m,n} = \tilde{S}_{m,n}\frac{\beta^{-m+n}+\beta^{m-n}}{2}, \qquad Q_{m,n} = \tilde{S}_{m,n}\frac{\beta^{-m+n}-\beta^{m-n}}{2}. \tag{S64}$$

Take Eqs. (S64), (S12), and (S13) into Eq. (S24), we find that the β's leading order of the QFI is $\beta^{4N-4}(\int_0^t dy|\tilde{S}_{N,1}|^2)^2$ when $\int_0^t dy|\tilde{S}_{N,1}|^2 \neq 0$. Therefore $F_\eta \propto \beta^{4N-4}$.